Model study of the impacts of future climate change on the hydrology of Ganges-Brahmaputra-Meghna (GBM) basin

Muhammad Masood[1,2], Pat J.-F. Yeh[3], Naota Hanasaki[4] and Kuniyoshi Takeuchi[1]

[1]{International Centre for Water Hazard and Risk Management (ICHARM), PWRI, Tsukuba, Japan}

[2]{National Graduate Institute for Policy Studies (GRIPS), Tokyo, Japan}

[3]{National University of Singapore, Singapore}

[4]{National Institute for Environmental Studies, Tsukuba, Japan}

Correspondence to: Muhammad Masood (masood35bd@yahoo.com)

Abstract

The intensity, duration, and geographic extent of floods in Bangladesh mostly depend on the combined influences of three river systems, Ganges, Brahmaputra and Meghna (GBM). In addition, climate change is likely to have significant effects on the hydrology and water resources of the GBM basins and might ultimately lead to more serious floods in Bangladesh. However, the assessment of climate change impacts on basin-scale hydrology by using well-calibrated hydrologic modelling has seldom been conducted for GBM basins due to the lack of data for model calibration and validation. In this study, a macro-scale hydrologic model H08 has been applied regionally over the basin at a relatively fine grid resolution (10 km) by integrating the fine-resolution (~0.5 km) DEM data for accurate river networks delineation. The model has been calibrated via analysing model parameter sensitivity and validated based on a long-term observed daily streamflow data. The impacts of climate change (considering high emissions path) not only on the runoff, but also on the basin-scale hydrology including evapotranspiration, soil moisture and net radiation have been assessed in this study by using 5 GCMs of CMIP5 through three time-slice experiments; present-day (1979–2003), near-future (2015-2039) and far-future (2075–2099) periods. Results show that, by the end of 21st century

(a) the entire GBM basin is projected to be warmed by ~4.3°C (b) the changes of mean precipitation are projected to be +16.3%, +19.8% and +29.6%, and the changes of mean runoff to be +16.2%, +33.1% and +39.7% in the Brahmaputra, Ganges and Meghna basins, respectively (c) evapotranspiration is projected to increase significantly for the entire GBM basins (Brahmaputra: +16.4%, Ganges: +13.6%, Meghna: +12.9%) due to increased net radiation (Brahmaputra: +5.6%, Ganges: +4.1%, Meghna: +4.4%) as well as warmer air temperature. Changes of hydrologic variables will be larger in dry season (November-April) than that in wet season (May-October). Amongst three basins, Meghna shows the highest increase in runoff which indicates higher possibility of flood occurrence in this basin. The uncertainty due to the specification of key model parameters in predicting hydrologic quantities, has also been analysed explicitly in this study, and it is found that the uncertainty in estimated runoff, evapotranspiration and net radiation is relatively low. However, the uncertainty in estimated soil moisture is rather large (coefficient of variation ranges from 14.4 to 31% among three basins).

1 Introduction

Bangladesh is situated in the active delta of the world's three major rivers, the Ganges, Brahmaputra and Meghna. Due to its unique geographical location, the occurrence of water-induced disasters is a regular phenomenon. In addition, the anticipated change in climate is likely to lead to an intensification of the hydrological cycle and to have a major impact on overall hydrology of these basins and ultimately lead to increase the frequency of water-induced disasters in Bangladesh. However, the intensity, duration, and geographic extent of floods in Bangladesh mostly depend on the combined influences of these three river systems. Previous studies revealed that flood damages have become more severe and devastating when more than one flood peaks in these three river basins coincide (Mirza, 2003;Chowdhury, 2000).

The Ganges-Brahmaputra-Meghna (hereafter referred to as GBM) river basin with a total area of about 1.7 million km^2 (FAO-AQUASTAT, 2014;Islam et al., 2010) encompasses a number of countries including parts of China, India, Nepal, Bhutan and Bangladesh (Fig. 1). Major characteristics of the GBM rivers have been presented in Table 1. This river system is the third largest freshwater outlet in the world to the oceans (Chowdhury and Ward, 2004). During the extreme floods, over 138 700 $m^3 s^{-1}$ of water flows into the Bay of Bengal through

a single outlet, which is the largest intensity in the world even exceeding that of the Amazon discharge into the sea by about 1.5 times (FAO-AQUASTAT, 2014). The GBM river basin is unique in the world in terms of diversified climate. For example, the Ganges river basin is characterized by low precipitation (760–1020 mm $year^{-1}$) in the northwest upper region and high precipitation (1520–2540 mm $year^{-1}$) along the coastal areas. High precipitation zones and dry rain shadow areas are located in the Brahmaputra river basin, whereas the world's highest precipitation (~5690 mm $year^{-1}$) area is situated in the Meghna River basin (FAO-AQUASTAT, 2014).

Several studies have focused on the rainfall and discharge relationships in the GBM basin by (1) identifying and linking the correlation between basin-scale discharge and the El Nino-southern oscillation (ENSO) and sea surface temperature (SST) (Chowdhury and Ward, 2004;Mirza et al., 1998;Nishat and Faisal, 2000), (2) analysing available observed or reanalysis data (Chowdhury and Ward, 2004, 2007;Mirza et al., 1998;Kamal-Heikman et al., 2007), and (3) evaluating historical data of flood events (Mirza, 2003;Islam et al., 2010). Various statistical approaches were used in most of these studies instead of conducting hydrologic model simulations. In recent years, a number of global-scale hydrologic modelling studies (Haddeland et al., 2011;Haddeland et al., 2012;Pokhrel et al., 2012) have been reported. Although their modelling domains include the GBM basin, these global-scale simulations are not well constrained due to the lack of calibration at the basin scale.

Few studies have been conducted to investigate the impact of climate change on the hydrology and water resources of the GBM basins (Immerzeel, 2008;Kamal et al., 2013;Biemans et al., 2013;Gain et al., 2011;Ghosh and Dutta, 2012;Mirza and Ahmad, 2005a). In most of these studies, future streamflow is projected on the basis of linear regression between rainfall and streamflow derived from historical data (Immerzeel, 2008;Chowdhury and Ward, 2004;Mirza et al., 2003). Immerzeel (2008) used the multiple regression technique to predict streamflow at the Bahadurabad station (the outlet of Brahmaputra basin) under future temperature and precipitation conditions based on the statistically downscaled GCM output. However, since most of the hydrologic processes are nonlinear, they cannot be predicted accurately by using empirical regression equations derived from historical data and then extrapolating to the future conditions with the non-stationary changes. The alternative for the assessment of climate change impacts on basin-scale hydrology is by using well-calibrated hydrologic modelling, but this has rarely been conducted for the GBM basin due to the lack of

data for model calibration and validation. Ghosh and Dutta (2012) applied a physically-based, macro-scale distributed hydrologic model to study the change of future flood characteristics at the Brahmaputra basin, but their study domain only focused on the regions inside India rather than the entire basin. Gain et al. (2011) estimated the future trends of the low and high flows in the lower Brahmaputra basin using outputs from a global hydrologic model forced by multiple GCM outputs (grid resolution: 0.5^{o}). Instead of calibrating the model, the simulated future streamflow was weighted against the observations to assess the impacts due to climate change.

In contrast to the above studies, in this study a hydrologic model simulation will be conducted. The calibration and validation will be based on a rarely obtained long-term (1980-2001) observed daily streamflow dataset in the GBM basin provided by the Bangladesh Water Development Board (BWDB). Relative to previous studies over the GBM basin, it is believed that the availability of this unique long-term streamflow data can lead to more precise estimation of model parameters and hence more accurate simulation of hydrological processes as well as more reliable future projection of the hydrology over the GBM basin.

The objective of this study is to (1) setup a hydrologic model by calibration and validation with long-term observed daily discharge data that can reproduce the long-term hydrographs of this basin reliably, and to (2) study the impact of future climate changes on the basin-scale hydrology of this basin. A global-scale hydrologic model H08 (Hanasaki et al., 2008;Hanasaki et al., 2014) is applied regionally over the GBM basin at a relatively fine grid resolution (10 km) by integrating the fine-resolution (~0.5 km) DEM data for the accurate river networks delineation. The hourly atmospheric forcing dataset from the Water and Global Change (WATCH) model-inter-comparison project (Weedon et al., 2011) (hereafter referred to as WFD (WATCH Forcing Dataset)) is used for the historical simulations in this study. WFD is considered as one of the best available global climate forcing datasets to provide accurate representation of meteorological events, synoptic activity, seasonal cycles and climate trends (Weedon et al., 2011). The studies by Lucas-Picher et al. (2011) and Siderius et al. (2013) found that for the South Asia and the Ganges, respectively, the WFD rainfall is consistent with the observed APHRODITE data (Yatagai et al., 2012) -a gridded (0.25°) rainfall product for the South Asia region developed based on a large number of rain gauge data. For the future simulations, the hydrologic model is forced by climate output from simulations of high emissions scenario (RCP 8.5 of all model except MRI-AGCM3.2S which

includes SRES A1B scenario) from 5 different coupled atmosphere–ocean general circulation models and earth system models (hereafter referred to as GCMs), all participating in the Coupled Model Intercomparison Project Phase 5 (CMIP5) (Taylor et al., 2012). In order to be consistent with the historical data, the monthly correction factor (i.e. the ratio between the basin-scale long-term monthly mean precipitation of the WFD data and that of the GCM data for each month) for each basin is applied to each GCM's precipitation forcing data. Several time-slice experiments are performed for the present-day (1979–2003), near-future (2015-2039) and far-future (2075–2099) periods.

The modelling study in the present study makes advances from previous studies in three aspects. First, a hydrologic model H08 (Hanasaki et al., 2008) is used which has been demonstrated as suitable for large-scale analyses. The model is well calibrated for the GBM basin via analysing model parameter sensitivity from the parameter-sampling simulations. The model has been validated against daily observed streamflow satisfactorily. Moreover, the uncertainty due to the determination of key model parameters in predicting hydrologic quantities, which has seldom been performed in previous studies, is analysed explicitly in this study. Second, three large basins of GBM and their spatial variability are studied in this study which benefit the analysis of their combined influences on the large-scale hydrologic floods and droughts occurred in Bangladesh as extensively reported in literature (Chowdhury, 2000;Mirza, 2003). Finally, the impacts of climate change not only on the discharge but also on the basin-scale hydrology including evapotranspiration, soil moisture and net radiation, are assessed in this study, whereas in most previous studies the climate change impact on streamflow was often the only focus.

The paper is organized into five sections as follows. A brief description of the data and the hydrologic model used is presented in Sect. 2. Section 3 presents the methodology of model setup as well as the results from the model parameter sensitivity analysis. Results and discussion are presented in Sect. 4. Finally, important conclusions of this study are summarized in Section 5.

2 Data and Tools

2.1. Meteorological Forcing datasets

The WATCH Forcing Data set (WFD) (Weedon et al., 2011) is used to drive the H08 model for the historical simulation. The WFD variables, including rainfall, snowfall, surface pressure, air temperature, specific humidity, wind speed, long-wave downward radiation, and shortwave downward radiation were taken from the ERA-40 reanalysis product of the European Centre for Medium Range Weather Forecasting (ECMWF). The one-degree resolution ERA40 reanalysis data were interpolated into the half-degree resolution on the Climate Research Unit of the University of East Anglia (CRU) land mask, adjusted for elevation changes where needed and bias-corrected using monthly observations. For detailed information on the WFD, see Weedon et al. (2011) and Weedon et al. (2010). The albedo values are based on the monthly albedo data form the Second Global Soil Wetness Project (GSWP2).

2.2. Hydrologic data

Observed river water level (daily) and discharge (weekly) data from 1980 to 2012 for the hydrological stations located inside the Bangladesh (the outlets of three basins shown in Fig. 1, i.e. the Ganges basin at Hardinge Bridge, the Brahmaputra basin at Bahadurabad, and the Meghna basin at Bhairab Bazar) were provided by the Hydrology Division, Bangladesh Water Development Board (BWDB). River water levels were regularly measured 5 times a day (at 6 am, 9 am, 12 pm, 3 pm and 6 pm) and discharges were measured weekly by the velocity-area method. Since the Brahmaputra River is highly braided, the discharge measurement at Bahadurabad was carried out on multiple channels. In contrast, the Meghna River at Bhairab Bazar is seasonally tidal - after withdrawal of the monsoon the river at this station becomes tidal, and from December to May the river shows both a horizontal and a vertical tide (Chowdhury and Ward, 2004). Under this condition, during the dry season, tidal discharge measurements were made at this station once per month. Daily discharges of Ganges and Brahmaputra River were calculated from the daily water level data by using the rating equations developed by the Institute of Water Modelling (IWM) (IWM, 2006). Rating equation for the Meghna River was not reported in literature. In this study an attempt was made to develop the rating equation for the Meghna basin. Discharge (monthly) data of three

more stations (Farakka, Pandu, Teesta) located at upstream of these basins (Fig. 1) were collected from the Global Runoff Data Centre (GRDC), which were used for validation.

2.3. Topographic Data

DEM data were collected from the HydroSHEDS (Hydrological data and maps based on SHuttle Elevation Derivatives at multiple Scales) (HydroSHEDS, 2014). It offers a suite of geo-referenced data sets (vector and raster), including stream networks, watershed boundaries, drainage directions, and ancillary data layers such as flow accumulations, distances and river topology information (Lehner et al., 2006). The HydroSHEDS data were derived from the elevation data of the Shuttle Radar Topography Mission (SRTM) at a ~0.5 km resolution. Preliminary quality assessments indicate that the accuracy of HydroSHEDS significantly exceeds that of existing global watershed and river maps (Lehner et al., 2006).

2.4. GCM data

Climate data from 5 CMIP5 climate models; MIROC5, MIROC-ESM, MRI-CGCM3, HadGEM2-ES under the RCP 8.5 representative concentration pathway and MRI-AGCM3.2S under the SRES A1B (Appendix B, Table B1) have been used for future simulation. The climate data has been interpolated from native climate model resolution (ranging from $0.25\times 0.25^{\circ}$ to $2.8\times 2.8^{\circ}$) to $5\times 5'$ (~10 km-mesh) using linear interpolation (nearest four point). In order to be consistent with the historical data, the bias of precipitation forcing data of each GCM has been corrected by multiplying the monthly correction factor equal to the ratio between the basin-averaged long-term mean precipitation from a GCM and that from WFD for each of the twelve months in each GBM basins. Among these GCMs, MRI-AGCM3.2S (where the 'S' refers to the "super-high resolution") provides higher resolution (20 km) atmospheric forcing data which shows improvements in simulating heavy precipitation, global distribution of tropical cyclones, and the seasonal march of East Asian summer monsoon (Mizuta et al., 2012). Therefore, climate change impacts on the south Asia were assessed in several recent studies by using the MRI-AGCM3.2S dataset (Rahman et al., 2012;Endo et al., 2012;Kwak et al., 2012).

2.5. Hydrologic Model: H08

H08 is a macro-scale hydrological model developed by Hanasaki et al (2008) which consists of six main modules: land surface hydrology, river routing, crop growth, reservoir operation, environmental flow requirement estimation, and anthropogenic water withdrawal. For this study, only two modules, the land surface hydrology and the river routing are used. The land surface hydrology module calculates the energy and water budgets above and beneath the land surface as forced by the high temporal-resolution meteorological data.

The runoff scheme in H08 is based on the bucket model concept (Manabe, 1969), but differs from the original formulation in certain important aspects. Although runoff is generated only when the bucket is overfilled as in the original bucket model, H08 uses a "leaky bucket" formulation in which subsurface runoff occurs continually as a function of soil moisture. Soil moisture is expressed as a single-layer reservoir with the holding capacity of 15 cm for all the soil and vegetation types. When the reservoir is empty (full), soil moisture is at the wilting point (the field capacity). Evapotranspiration is expressed as a function of potential evapotranspiration and soil moisture (Eq. 2). Potential evapotranspiration and snowmelt are calculated from the surface energy balance (Hanasaki et al., 2008).

Potential evaporation E_P is expressed in this model as

$$E_P(T_S) = \rho C_D U(q_{SAT}(T_S) - q_a) \quad (1)$$

.

Where ρ is the density of air, C_D is the bulk transfer coefficient U is the wind speed, q_{SAT} (T_S) is the saturated specific humidity at surface temperature, and q_a is the specific humidity. Evaporation from a surface (E) is expressed as

$$E = \beta E_P(T_S) \quad (2)$$

where

$$\beta = \begin{cases} 1 & 0.75W_f \le W \\ W/W_f & W < 0.75W_f \end{cases} \quad (3)$$

where W is the soil water content and W_f is the soil water content at field capacity (fixed at 150 kg m^{-2}).

Surface runoff (Q_s) is generated whenever the soil water content exceeds the field capacity:

$$Q_{\mathrm{s}} = \begin{cases} W - W_{\mathrm{f}} & W_{\mathrm{f}} < W \\ 0 & W \le W_{\mathrm{f}} \end{cases} \quad (4)$$

Subsurface runoff (Q_{sb}) is incorporated to the model as

$$Q_{\mathrm{sb}} = \frac{W_{\mathrm{f}}}{\tau}\left(\frac{W}{W_{\mathrm{f}}}\right)^{\gamma} \quad (5)$$

Where τ is a time constant and γ is a parameter characterizing the degree of nonlinearity of Q_{sb}. These two parameters are calibrated in this study as described later in Sect. 3.1.

The river module is identical to the Total Runoff Integrating Pathways (TRIP) model (Oki and Sud, 1998). The module has a digital river map covering the whole globe at a spatial resolution of 1^{o} (~111 km). The land–sea mask is identical to the GSWP2 meteorological forcing input. Effective flow velocity and meandering ratio are set as the default values at 0.5 m s^{-1} and 1.5, respectively. The module accumulates runoff generated by the land surface model and routes it downstream as streamflow. However, for this study a new digital river map of the GBM basin with the spatial resolution of ~10 km is prepared. Effective flow velocity and meandering ratio have been calibrated respectively for the three basins.

3 Methodology: model setup and simulation

Figure 2 presents the methodology used in this study from model setup to the historical and future simulations. A H08 simulation with the 10-km (5 min) resolution is calibrated to find the optimal parameter sets by using the parameter-sampling simulation technique, and validated with observed daily streamflow data. The default river module of H08 uses the digital river map from TRIP (Oki and Sud, 1998) with the global resolution of 1º (~111 km), which is too course for the regional simulation in this study with the 10-km resolution. Therefore, a new digital river map of the 10-km resolution is prepared by integrating the finer-resolution (~0.5 km) DEM data.

3.1. Parameter sensitivity

The parameter-sampling simulation is conducted to investigate the sensitivity of the H08 model parameters to model simulation results. The most sensitive parameters in H08 include the root-zone depth d [m], the bulk transfer coefficient C_{D} [-] controlling the potential evaporation (Eq. 1), and the parameters sensitive to subsurface flow, that is, τ [day] and γ [-]

(Eq. 5) (Hanasaki et al., 2014), hence they are treated as calibration parameters in this study. The parameter τ is a time constant determining the daily maximum subsurface runoff. The parameter γ is a shape parameter controlling the relationship between subsurface flow and soil moisture (Hanasaki et al., 2008). Their default parameter values in H08 are 1 m for d, 0.003 for C_D, 100 days for τ, and 2 for γ. For each of these four parameters, five different values are selected from their feasible physical ranges. The parameter-sampling simulations of the H08 model were run by using all the combinations of four parameters, which consist of a total of 5^4 (=625) simulations all conducted by using the same 11-year (1980–1990) atmospheric forcing data of WFD.

Figure 3 plots the 11-year long-term average seasonal cycles of simulated total runoff, surface runoff and sub-surface runoff of the Brahmaputra basin. Each of the five lines in each panel represents the average of 5^3 (=125) runs with one of the 4 calibration parameters fixed at a given value. As shown, the overall sensitivity of selected model parameters to the flow partitioning is high. When d is low, surface runoff is high (due to higher saturated fractional area) (Fig. 3 b). As d increases, sub-surface runoff increases and surface runoff decreases (Fig. 3 c and b). Due to these compensating effects, the effect of d on the total runoff becomes more complex: from March to August, higher d causes lower total runoff, but the trend is reversed from August on for the Brahmaputra basin. Similar behaviours can be observed for the other two basins (figure not shown).

The parameter C_D is the bulk transfer coefficient in the calculation of potential evaporation (Eq. 1), thus its effect on runoff is relatively small (Fig. 3d-f). However, higher C_D causes more evaporation and hence lower (both surface and sub-surface) runoff (Eq. 1 and Eq. 2). The sensitivity of parameter γ to runoff is also smaller than d and τ. As γ increases, surface runoff increases and sub-surface runoff decreases (Fig. 3h, i). The overall sensitivity of γ to the total runoff becomes negligible due to the compensating effects (Fig. 3g).

As shown in Eq. (5) and Fig. 3k-l, the parameter τ has a critical impact on the surface and sub-surface flow partitioning. A larger τ corresponds to larger surface runoff and hence smaller sub-surface runoff (Fig. 3k-l), but it has relatively a small impact on total runoff (Fig. 3j).

These four calibration parameters have the combined influences on total runoff partitioning as well as simulations of other hydrologic variables. To summarize, (1) the sensitivity of d on the total runoff is complex: the trend is reversed between the two halves of a year; (2) parameters d and τ have a significant impact on flow partitioning whereas C_D and γ have less

sensitivity to runoff simulation; (3) The influence of d and τ is reversed between surface and sub-surface runoff: surface runoff increases as d decreases and τ increases.

Figure 4e plots the uncertainty bands of the simulated discharges by using 10 optimal parameter combinations according to the Nash-Sutcliffe coefficient of efficiency (NSE) (Nash and Sutcliffe, 1970). It is observed that the spread of uncertainty band is located mainly around the low flow period (dry season from November to March) over the Brahmaputra basin (Fig. 4e). No surface runoff is generated in dry season when the soil moisture is lower than the field capacity (Eq. 4 and Fig. 3b). It is noted from the 10 optimal parameter combinations that the optimal τ is 150, C_D is 0.001, d and γ range from 3 to 5 and 1.0 to 2.5, respectively. The spread of the uncertainty bands is mainly due to the variations of the d and γ. As d increases, the sub-surface runoff increases (Fig. 3c and Fig. 4e). On the other hand, in the case of the Ganges and Meghna basin the spread of uncertainty bands are observed through the entire period of a year (in low flow as well as in peak flow regimes). Among the 10 optimal parameter combinations for Ganges (Meghna) it is found that parameter C_D is 0.008 (0.008), τ is 150 (50), d and γ range from 4 to 5 (4 to 5) and 2.5 to 4 (1.5 to 2), respectively. In the dry period when surface runoff is nearly zero, sub-surface runoff increases as d increases. A higher C_D causes higher evaporation which influences runoff as well (Eq. 1). As discussed earlier, the influence of d on the total runoff is complex which results in the variation of simulated runoff throughout the year. The spread of the uncertainty bands is large in the peak flow period as the sensitivity of both surface and sub-surface runoff is also large with respect to the value of d (not shown).

3.2. Calibration and Validation

The historical simulation from 1980 to 2001 is divided into two periods with the first half (1980-1990) as the calibration period and the second half (1991-2001) as validation. Basic information and characteristics (location, drainage area, and periods of available observed data) of the 6 validation stations in the GBM are summarized in Table 3. Model performance is evaluated by comparing observed and simulated daily streamflow by the Nash–Sutcliffe efficiency (NSE) (Nash and Sutcliffe, 1970), the optimal objective function for assessing the overall fit of a hydrograph (Sevat and Dezetter, 1991). A series of sensitivity analysis of H08 parameters was conducted from which the 10 sets of the optimal parameter are determined by using the parameter-sampling simulation as discussed earlier, and these parameter sets will be used to quantify the uncertainty in both historical and future simulations in the following.

Figure 4 plots the daily hydrograph comparisons at the outlets of three river basins with the corresponding daily observations for both calibration and validation periods. The obtained NSE for the calibration (validation) period is 0.84 (0.78), 0.80 (0.77), and 0.84 (0.86), while the percent bias (PBIAS) is 0.28% (6.59%), 1.21% (2.23%) and -0.96% (3.15%) for the Brahmaputra, Ganges, and Meghna basins, respectively. For all basins, the relative Root-Mean Square Error (RRMSE), the correlation coefficient (cc), and the coefficient of determination (R^2) for the calibration (validation) period ranges from 0.32 to 0.60 (0.32 to 0.59), 0.91 to 0.93 (0.89 to 0.94) and 0.82 to 0.86 (0.79 to 0.88), respectively. These statistical indices suggest the model performance is overall satisfactory. To further evaluate the model performance at upstream stations, the observed monthly discharge data at three upstream stations (Farakka, Pandu, Teesta) are collected from the Global Runoff Data Centre (GRDC) to compare with model simulations. The results are summarized presented in Appendix A.

4 Results and Discussion

The calibrated H08 model is applied to simulate for the following three time-slices periods, present (1979–2003), near-future (2015-2039) and the far-future (2075–2099). For the present simulations, both the WFD and GCMs climate forcing data were used. For the future simulation, only the GCMs forcing data are used. Simulation results for the future periods are then compared with the present period (1979–2003) simulation forced by GCM to assess the effect of climate change on the hydrology and water resources of GBM in terms of precipitation, air temperature, evapotranspiration, soil moisture and net radiation. The results are presented in the following.

4.1. Seasonal cycle

Figure 5 plots the 22-year (1980-2001) mean seasonal cycles of the climatic (from WFD forcing) and hydrologic (from the model simulation) quantities averaged over the three basins (The corresponding mean annual amounts of these variables are presented in Table 4). Also shown in Figure 5 is the Box-and-Whisker plot showing the range of variability within each of the twelve months. The interannual variation of precipitation in Brahmaputra and Meghna is high from May to September (Fig. 5a,c) whereas in Ganges it is from June to October. However, the magnitudes of precipitation differed substantially among three basins. The Meghna has significantly higher precipitation than other two basins (Table 4), also the

maximum (monthly) precipitation during 1980-2001 occurs in May with the magnitude of 32 mm day^{-1}, while those in Brahmaputra and Ganges occurs in July with the magnitudes of 15 mm day^{-1} and 13 mm day^{-1}, respectively. Moreover, the seasonality of runoff in all three basins corresponded very well with that of precipitation. Runoff (Fig. 5j-l) in Ganges was much lower (the maximum of 4.3 mm day^{-1} in August) than the other two basins (the maximum of 9.3 mm day^{-1} in Brahmaputra and 15.9 mm day^{-1} in Maghna, both in July). In addition, ET in the Brahmaputra is significantly lower (annual total 251 mm) than in the other two basins (annual total 748 mm in Ganges and 1000 mm in Meghna). Lower ET in the Brahmaputra basin is likely due to its cooler air temperature, higher elevation and less vegetated area. The basin-averaged Normalized Difference Vegetation Index (NDVI) of the Brahmaputra is 0.38, whereas for the Ganges and Meghna, NDVI are 0.41 and 0.65, respectively (NEO, 2014). However, the patterns of seasonal variability of ET in Brahmaputra and Meghna are quite similar, except there is a drop in July in Brahmaputra (Fig. 5m-o). ET is relatively stable from May to October in Brahmaputra and Meghna (which suggests ET is at the potential rate) in contrast to that in Ganges where the ET does not reach the peak until September. Finally, both the pattern and magnitude of seasonal soil moisture variations are rather different among three basins (Fig. 5p-r). However, the peak of soil moisture occurs in August in all three basins.

Figure 5d-f present the 22-year mean seasonal cycle of basin average air temperature (Tair). Brahmaputra is much cooler (mean temperature 9.1°C) than Ganges (21.7°C) and Meghna (23.0°C). Figure 5g-i plot the mean seasonal cycle of net radiation averaged over these three basins. The seasonal pattern of net radiation is similar, but the magnitude differs significantly among three basins: The average net radiation is approximately 31, 74 and 84 W m^{-2} in Brahmaputra, Ganges and Meghna, respectively, while the maximum net radiation is about 47, 100 and 117 W m^{-2}, respectively (Table 4).

4.2. Correlation between meteorological and hydrological variables

Figure 6 presents the scatter plots and the correlation coefficients (cc) between the monthly meteorological and hydrological variables in three river basins. Three different colours represent three different seasons: dry/winter (November-March), pre-monsoon (April-June), and monsoon (July-October). From this plot, the following summary can be drawn. Total runoff and surface runoff of Brahmaputra have stronger correlation (cc= 0.95 and 0.97, both are statistically significant at $p<0.05$) with precipitation than in other two basins. However,

subsurface runoff in Brahmaputra has weaker correlation (cc=0.62, $p<0.05$) with precipitation than that in Ganges (cc=0.75, $p<0.05$) and Meghna (cc=0.77, $p<0.05$). These relationships imply that the deeper soil depths enhance the correlation between subsurface runoff and precipitation. The deeper root-zone soil depth (calibrated d = 5m) in Meghna generates more subsurface runoff (69% of total runoff) than other two basins. Soil moisture in Meghna also shows stronger correlation (cc=0.87, $p<0.05$) with precipitation than that in Brahmaputra (cc=0.77, $p<0.05$) and Ganges (cc=0.82, $p<0.05$).

The relationships of evapotranspiration with various atmospheric variables (radiation, air temperature) and soil water availability are rather complex (Shaaban et al., 2011). Different methods for estimating potential evapotranspiration (PET) in different hydrological models may also be a source of uncertainty (Thompson et al., 2014). However, the ET scheme in the H08 model uses the bulk formula where the bulk transfer coefficient is used to calculate turbulent heat fluxes (Haddeland et al., 2011). In estimating PET (and hence ET), H08 uses humidity, air temperature, wind speed and net radiation. Figure 6 presents the correlation of ET with different meteorological variables in three basins. The ET in the Brahmaputra has a significant correlation with precipitation, air temperature, specific humidity and net radiation with the correlation coefficients (cc) range from 0.70 to 0.89 (all of which are statistically significant at $p<0.05$). The correlation of ET in Meghna with the meteorological variables are also relatively strong (cc range from 0.61 to 0.80, $p<0.05$) except for the net radiation (cc=0.44, $p<0.05$). However, ET in Ganges has a weak correlation with the meteorological variables (cc from 0.29 to 0.59, $p<0.05$). A weaker correlation of ET with the meteorological variables is likely attributed to the over-estimation of actual ET in the Ganges, because the up-stream water use (which is larger in Ganges) may be incorrectly estimated as ET by the H08 model to ensure water balance.

4.3. Interannual variability

Figure 7 presents the interannual variability of meteorological and hydrologic variables from using 5 different GCMs and that of the multi-model mean (shown by the thick blue line) for three basins. It can be seen from the figure that the magnitude of interannual variations of each individual GCM are noticeably larger than that of the multi-model mean. However, the long-term trends in the meteorological and hydrologic variables of the multi-model mean are generally similar to that of each GCMs. Figure 7a1-a3 show the long-term trend in precipitation is not pronounced for all three basins, but its interannual variability is rather

large for each GCM. Among 5 GCMs used, the precipitation of MRI-AGCM3 has the largest interannual variability (particularly in the Ganges and Meghna basin). A clear increasing trend in air temperature can be observed for all three basins. As there is strong correlation between precipitation and runoff (Fig. 6), the interannual variability of them are similar. There is no clear trend that can be observed for ET in each basin from the present to the near-future period. However, in the far-future a notable increasing trend is observed for all basins (Fig. 7e1-e3). Figure 7f1-f3 plots the interannual variability of soil moisture. Since there are no clear trends (from the present to the near-future period) identified from precipitation and evapotranspiration, the effect of climate change on soil moisture is relatively less pronounced from this modelling study.

4.4. Projected mean changes

The changes in the seasonal cycles of hydro-meteorological variables in the two projected periods (2015-2039 and 2075–2099) are comparing with that in the reference period (1979-2003). All the results presented here are from the multi-model mean of all simulations driven by the climate forcing data from 5 GCMs for both reference and future periods. The solid lines in Fig. 8 represent the monthly averages and the dashed lines represent the upper and lower bounds of the uncertainty bands as determined from the 10 simulations using the 10 optimal parameter sets (identified by ranking the Nash–Sutcliffe efficiency (NSE)). Figure 9 plots the corresponding percentage changes and Table 5 summarizes these relative changes in the hydro-meteorological variables over three basins on the annual and 6-month (dry season and wet season) basis.

4.4.1. Precipitation

Considering high emission scenario, by the end of 21st century the long-term mean precipitation is projected to increase by 16.3%, 19.8% and 29.6% in the Brahmaputra, Ganges and Meghna basin, respectively (Table 5), in agreement with previous studies which compared GCM simulation results over these regions. For example, Immerzeel (2008) estimated the increase of precipitation in the Brahmaputra basin as 22% and 14% under the SRES A2 and B2 scenarios, respectively. Endo et al. (2012) considered the SRES A1B scenario and estimated the country-wise increase in precipitation as 19.7% and 13% for Bangladesh and India respectively. Based on the present study, for the Brahmaputra and Meghna basins the change of precipitation in dry season (November-April) is 23% and 33.6%,

respectively, both are larger than the change in wet season (May-October) (Brahmaputra: 15.1%, Meghna: 29%) (Fig. 9b-c). However, the change of precipitation in dry season in Ganges (3.6%) is lower than that in wet season (21.5%).

4.4.2. Air temperature

The GBM basin will be warmer by the range of 1-4.3°C in the near-future (Brahmaputra: 1.2°C, Ganges: 1.0°C, Meghna: 0.7°C) and far-future (Brahmaputra: 4.8°C, Ganges: 4.1°C, Meghna: 3.8°C), respectively (Table 5). According to the projected changes, the cooler Brahmaputra basin will be significantly warmer by the maximum increase up to 5.9°C in February (Fig. 9d). In Immerzeel (2008), the increase of air temperature in Brahmaputra is projected (under the SRES A2 and B2 scenarios) as 2.3°C ~3.5°C by the end of 21st century. However, The rate of increase over the year is not uniform for all these basins. Temperature will increase more in winter than that in summer (Fig. 9d-f). Therefore, a shorter winter and an extended spring can be expected in the future of the GBM basin, which may significantly affect the crop growing season as well.

4.4.3. Runoff

Long-term mean runoff is projected to be increased by 16.2%, 33.1% and 39.7% in Brahmaputra, Ganges and Meghna, respectively by the end of the century (Table 5). Percentage increase of runoff in Brahmaputra will be quite large in May (about 36.5%), which may be due to the increase of precipitation and also smaller evapotranspiration caused by lower net radiation (Fig. 9g, m). In response to seasonally varying degrees of changes in air temperature, net radiation and evaporation, the changes of runoff in wet season (May-October) (Brahmaputra: 20.3%, Ganges: 36.3%, Meghna: 41.8%) are larger than that in dry season (November-April) (Brahmaputra: 2.9%, Ganges: -2.3%, Meghna: 24.2%) (Fig. 9j-k). Runoff in Meghna shows larger response to precipitation increase, which could lead to higher possibility of floods in this basin and prolonged flooding conditions in Bangladesh. These findings are in general consistent with previous findings. Mirza (2002) reported that the probability of occurrence of 20-year floods are expected to be higher in the Brahmaputra and Meghna Rivers than in Ganges River. However, Mirza et al. (2003) found future change in the peak discharge of the Ganges River (as well as the Meghna River)is expected to be larger than that of the Brahmaputra River.

4.4.4. Evapotranspiration

It can be seen from Fig. 9m-o that the change of ET in near-future is relative low, but increases to be quite large by the end of the century (Brahmaputra: 16.4%, Ganges: 13.6%, Meghna: 12.9%). This is due to the increase of net radiation (Brahmaputra: 5.6%, Ganges: 4.1%, Meghna: 4.4%) as well as the warmer air temperature. Following the seasonal patterns of radiation (Fig. 9g-i) and air temperature (Fig. 9d-f), the change of ET will be considerably larger in dry season (November-April) (Brahmaputra: 25.6%, Ganges: 19.3%, Meghna: 18.2%) than that in wet season (May-October) (Brahmaputra: 12.9%, Ganges: 10.9%, Meghna: 10.5%).

4.4.5. Soil moisture

Soil moisture is expressed in terms of the water depth per unit area within the spatially varying soil depths (3 ~ 5 m). The change of soil moisture (ranges from 1.5 ~ 6.9% in the far-future) is lower compared to other hydrological quantities, except for the Meghna in April where the soil moisture is projected to increase by 22%. However, the associated uncertainties through all seasons are relatively high compared to other variables (Fig. 8f1-f3).

4.4.6. Net radiation

Net radiation is projected to be increased by >4% for all the seasons except summer in the entire GBM basin by the end of the century (Figure 9g-i). Due to the increase in the future air temperature, the downward long-wave radiation will increase accordingly and lead to the increase in net radiation. However, the change of net radiation in the far-future period is larger in dry season (Brahmaputra: 10.3%, Ganges: 5.3%, Meghna: 6.5%) than wet season (Brahmaputra: 3.1%, Ganges: 3.4%, Meghna: 3%). For the near-future period, net radiation is projected to decrease by <1% through about all seasons due to the smaller increase in air temperature (~1°C) as well as decreased incoming solar radiation (not shown) in this basin.

4.5. Uncertainty in projection due to model parameters

In recent decades, along with the increasing computational power there has been a trend towards increasing complexity of hydrological models to capture natural phenomenon more precisely. However, the increased complexity of hydrological models does not necessarily improve their performance for unobserved conditions due to the uncertainty in the model parameters values (Carpenter and Georgakakos, 2006;Tripp and Niemann, 2008). An increase

in complexity may improve the calibration performance due to the increased flexibility in the model behaviour, but the ability to identify correct parameter values is typically reduced (Wagener et al., 2003). Multiple parameter sets can reproduce the observations with the similar accuracy. Another source of uncertainty comes from the assumption of stationary model parameters, which is one of the major limitations in modelling the effects of climate change. Model parameters are commonly estimated under the current climate conditions as a basis for predicting future conditions, but the optimal parameters may not be stationary over time (Mirza and Ahmad, 2005b). Therefore, the uncertainty in future projections due to model parameters specification can be critical (Vaze et al., 2010; Merz et al., 2011; Coron et al., 2012), although it is usually ignored in most climate change impact studies (Lespinas et al., 2014). Results obtained by Vaze et al. (2010) indicated that the model parameter can generally be used for climate impact studies when model is calibrated using more than 20-year of data and where the future precipitation is not more than 15% drier or 20% wetter than that in the calibration period. However, Coron et al. (2012) found a significant level of errors in simulations due to this uncertainty and suggested further research to improve the methods of diagnosing parameter transferability under the changing climate. For the purpose of minimizing this parameter uncertainty the average results from the 10 simulations using 10 optimal parameter sets are considered as the simulation result for the two future periods in this study. Also the propagating uncertainty in simulation results due to the uncertainty in mode parameters will be quantified and compared among various hydrologic variables in this study.

From Fig. 8 where the upper and lower bounds of the uncertainty of hydro-meteorological variables are plotted for all the simulation periods. It can be seen that the uncertainty band of runoff is relatively narrow, which indicates future runoff is well predictable through model simulations in this study. The uncertainty due to model parameters in runoff prediction is lower (the coefficient of variation (CV) ranges between 3 – 7.6% among three basins) than that of other hydrologic variables (Fig. 8d1-d3). In addition, from Fig. 4e it is observed that there is no significant uncertainty in simulated peak discharge for the Brahmaputra and Meghna River. Lower uncertainty in predicting runoff is highly desirable for climate change impact studies, for instance, the flood risk assessment where the runoff estimate (especially the peak flow) is the main focus. However, a relatively wide uncertainty band of runoff can be found in Ganges in wet season (Fig. 8d2), which might be due to that the upstream water use (diversion) in Ganges was not well represented in the model. Notice that the lower uncertainty

in runoff prediction relative to other variables is expected as the model is calibrated and validated against observed streamflow at the basin outlet. The uncertainty in ET prediction is also lower (CV: 3.6–11.3%; SD: 0.1–0.4), which can be related to the narrower uncertainty band of net radiation (CV: 1.8–8.6%; SD: 1.8–5.6). On the other hand, the prediction of soil moisture is rather uncertain for all three basins (CV: 14.4–31%; SD: 35–104). Large uncertainty in predicting soil moisture can be a serious issue significant in land use management and agriculture in particular, and this emphasizes the critical importance of having soil moisture observations for constraining model simulations in addition to the issues regarding the identifiability of model parameters.

5 Conclusions

This study presents model analyses of the climate change impact on Ganges-Brahmaputra-Meghna (GBM) basin focusing on (1) the setup of a hydrologic model by integrating the fine-resolution (~0.5 km) DEM data for the accurate river networks delineation to simulate at relatively fine grid resolution (10 km) (2) the calibration and validation of the hydrologic model with long-term observed daily discharge data and (3) the impacts of future climate changes in the basin-scale hydrology. The uncertainties in the future projection stemming from model parameter were also assessed. The time-slice numerical experiments were performed using the model forced by the climatic variables from 5 GCMs (all participating in the CMIP5) for the present-day (1979–2003), near-future (2015-2039) and the far-future (2075–2099) periods.

The following findings and conclusions were drawn from the model analysis:

- (a) The entire GBM basin is projected to be warmer by the range of 1-4.3°C in the near-future and far-future, respectively. And the cooler Brahmaputra basin will be warmer than the Ganges and Meghna. (b) Considering high emissions scenario, by the end of 21st century the long-term mean precipitation is projected to increase by +16.3, +19.8 and +29.6%, and the long-term mean runoff is projected to increase by +16.2, +33.1 and +39.7% in the Brahmaputra, Ganges and Meghna basin, respectively. (c) The change of ET in near-future is relative low, but increases to be quite large by the end of the century due to the increase of net radiation as well as the warmer air temperature. However, the change will be considerably larger in dry season than that in wet season. (d) The change of soil moisture is lower compared to other hydrological quantities.

- ✧ Over all, it is observed that climate change impact on the hydrology of the Meghna basin is larger than that of the other two basins. For example, in the near-future runoff of Meghna is projected to increase 19.1% whereas it is 6.7% and 11.3% for Brahmaputra and Ganges, respectively. In far-future larger increase of precipitation (29.6%) and lower increase of ET (12.9%) and consequently larger increase of runoff (39.7%) lead to higher possibility of floods in this basin.

- ✧ The uncertainty due to model parameters in runoff prediction is lower than that of other hydrologic variables. The uncertainty in ET prediction is also lower, which can be related to the narrower uncertainty band of net radiation. On the other hand, the prediction of soil moisture is rather uncertain for all three basins, which can be significant in land use management and agriculture in particular, and this emphasizes the importance of having soil moisture observations for model calibration.

However this study still has some limitations which can be addressed in future research; (a) all results presented here are basin-averaged. The basin-averaged large scale changes and trends are difficult to translate to regional and local scale impacts. Moreover, the changes in averages do not reflect the changes in variability and extremes, (b) anthropogenic and industrial water use in upstream are important factors in altering hydrologic cycle, however, which are not considered in present study due to data constraint, (c) urbanizing watersheds are characterized by rapid land use changes and associated land-scape disturbances can shift the rainfall–runoff relationships away from natural processes. Hydrological changes in future can also be amplified by changing land uses. However, in our study future changes of demography and land uses are not considered.

Acknowledgments. This study is supported by Public Works Research Institute (PWRI), Japan. The first author is indebted to the authority of Nippon Koei Co., Ltd, Japan for the grant from "The Kubota Fund". Also, thanks are given to A. Hasegawa, T. Sayama for help in data preparation and for suggestions, and to FFWC, BWDB for providing observed hydrological data.

References

Abrams, P.: River Ganges, available at: http://www.africanwater.org/ganges.htm (last access date: 13 July 2014), 2003.

Biemans, H., Speelman, L. H., Ludwig, F., Moors, E. J., Wiltshire, A. J., Kumar, P., Gerten, D., and Kabat, P.: Future water resources for food production in five South Asian river basins and potential for adaptation — A modeling study, Science of The Total Environment, 468–469, Supplement, S117-S131, doi:10.1016/j.scitotenv.2013.05.092, 2013.

BWDB: Rivers of Bangladesh, Bangladesh Water Development Board, Dhaka, 2012.

Carpenter, T. M., and Georgakakos, K. P.: Intercomparison of lumped versus distributed hydrologic model ensemble simulations on operational forecast scales, Journal of Hydrology, 329, 174-185, http://dx.doi.org/10.1016/j.jhydrol.2006.02.013, 2006.

Chowdhury, M. R.: An Assessment of Flood Forecasting in Bangladesh: The Experience of the 1998 Flood, Natural Hazards, 139–163, 2000.

Chowdhury, M. R., and Ward, M. N.: Hydro-meteorological variability in the greater Ganges-Brahmaputra-Meghna basins, International Journal of Climatology, 24, 1495-1508, 10.1002/joc.1076, 2004.

Chowdhury, M. R., and Ward, M. N.: Seasonal flooding in Bangladesh – variability and predictability, Hydrological Processes, 21, 335-347, 10.1002/hyp.6236, 2007.

Coron, L., Andréassian, V., Perrin, C., Lerat, J., Vaze, J., Bourqui, M., and Hendrickx, F.: Crash testing hydrological models in contrasted climate conditions: An experiment on 216 Australian catchments, Water Resources Research, 48, n/a-n/a, 10.1029/2011wr011721, 2012.

Endo, H., Kitoh, A., Ose, T., Mizuta, R., and Kusunoki, S.: Future changes and uncertainties in Asian precipitation simulated by multiphysics and multi–sea surface temperature ensemble experiments with high-resolution Meteorological Research Institute atmospheric general circulation models (MRI-AGCMs), Journal of Geophysical Research, 117, 10.1029/2012jd017874, 2012.

FAO-AQUASTAT: Ganges–Brahmaputra–Meghna River Basin, available at: http://www.fao.org/nr/water/aquastat/basins/gbm/index.stm (last access date: 19 April 2014), 2014.

Gain, A. K., Immerzeel, W. W., Sperna Weiland, F. C., and Bierkens, M. F. P.: Impact of climate change on the stream flow of the lower Brahmaputra: trends in high and low flows based on discharge-weighted ensemble modelling, Hydrology and Earth System Sciences, 15, 1537-1545, 10.5194/hess-15-1537-2011, 2011.

Ghosh, S., and Dutta, S.: Impact of climate change on flood characteristics in Brahmaputra basin using a macro-scale distributed hydrological model, J Earth Syst Sci, 121, 637-657, 10.1007/s12040-012-0181-y, 2012.

Haddeland, I., Clark, D. B., Franssen, W., Ludwig, F., Voß, F., Arnell, N. W., Bertrand, N., Best, M., Folwell, S., Gerten, D., Gomes, S., Gosling, S. N., Hagemann, S., Hanasaki, N., Harding, R., Heinke, J., Kabat, P., Koirala, S., Oki, T., Polcher, J., Stacke, T., Viterbo, P., Weedon, G. P., and Yeh, P.: Multimodel Estimate of the Global Terrestrial Water Balance: Setup and First Results, Journal of Hydrometeorology, 12, 869-884, 10.1175/2011jhm1324.1, 2011.

Haddeland, I., Heinke, J., Voß, F., Eisner, S., Chen, C., Hagemann, S., and Ludwig, F.: Effects of climate model radiation, humidity and wind estimates on hydrological simulations, Hydrology and Earth System Sciences, 16, 305-318, 10.5194/hess-16-305-2012, 2012.

Hanasaki, N., Kanae, S., Oki, T., Masuda, K., Motoya, K., Shirakawa, N., Shen, Y., and Tanaka, K.: An integrated model for the assessment of global water resources –Part 1: Model description and input meteorological forcing, Hydrol. Earth Syst. Sci., 1007–1025, 2008.

Hanasaki, N., Saito, Y., Chaiyasaen, C., Champathong, A., Ekkawatpanit, C., Saphaokham, S., Sukhapunnaphan, T., Sumdin, S., and Thongduang, J.: A quasi-real-time hydrological simulation of the Chao Phraya River using meteorological data from the Thai Meteorological Department Automatic Weather Stations, Hydrological Research Letters, 8, 9-14, 10.3178/hrl.8.9, 2014.

Hydrological data and maps based on SHuttle Elevation Derivatives at multiple Scales: http://hydrosheds.cr.usgs.gov/hydro.php, last access date: 19 April 2014.

Immerzeel, W.: Historical trends and future predictions of climate variability in the Brahmaputra basin, International Journal of Climatology, 28, 243-254, 10.1002/joc.1528, 2008.

Inomata, H., Takeuchi, K., and Fukami, K.: Development of a Statistical Bias Correction Method For Daily Precipitation Data of GCM20, Journal of Japan Society of Civil Engineers, 67, I_247-I_252, 10.2208/jscejhe.67.I_247, 2011.

Islam, A. S., Haque, A., and Bala, S. K.: Hydrologic characteristics of floods in Ganges-Brahmaputra-Meghna (GBM) delta, Natural Hazards, 54, 797-811, 2010.

IWM: Updating and Validation of North West Region Model (NWRM), Institute of Water Modelling, Bangladesh, 2006.

Kamal-Heikman, S., Derry, L. A., Stedinger, J. R., and Duncan, C. C.: A Simple Predictive Tool for Lower Brahmaputra River Basin Monsoon Flooding, Earth Interactions, 11, 1-11, 10.1175/ei226.1, 2007.

Kamal, R., Matin, M. A., and Nasreen, S.: Response of River Flow Regime to Various Climate Change Scenarios in Ganges-Brahmaputra- Meghna Basin, Journal of Water Resources and Ocean Science, 2, 15-24, 10.11648/j.wros.20130202.12, 2013.

Kwak, Y., Takeuchi, K., Fukami, K., and Magome, J.: A new approach to flood risk assessment in Asia-Pacific region based on MRI-AGCM outputs, Hydrological Research Letters, 6, 70-75, 10.3178/HRL.6.70, 2012.

Lehner, B., R-Liermann, C., Revenga, C., Vörösmarty, C., Fekete, B., Crouzet, P., Döll, P. et al.: High resolution mapping of the world's reservoirs and dams for sustainable river flow management. Frontiers in Ecology and the Environment. Source: GWSP Digital Water Atlas (2008). Map 81: GRanD Database (V1.0). Available online at http://atlas.gwsp.org

Lehner, B., Verdin, K., and Jarvis, A.: HydroSHEDS technical documentation v1.0, World

Wildlife Fund US, Washington, DC, 1-27, 2006.

Lespinas, F., Ludwig, W., and Heussner, S.: Hydrological and climatic uncertainties associated with modeling the impact of climate change on water resources of small Mediterranean coastal rivers, Journal of Hydrology, 511, 403-422, 10.1016/j.jhydrol.2014.01.033, 2014.

Lucas-Picher, P., Christensen, J. H., Saeed, F., Kumar, P., Asharaf, S., Ahrens, B., Wiltshire, A. J., Jacob, D., and Hagemann, S.: Can Regional Climate Models Represent the Indian Monsoon?, Journal of Hydrometeorology, 12, 849-868, 10.1175/2011jhm1327.1, 2011.

Manabe, S.: Climate and the ocean circulation – 1: The atmospheric circulation and the hydrology of the Earth's surface, Mon.Weather Rev., 97, 739–774, 1969.

Merz, R., Parajka, J., and Blöschl, G.: Time stability of catchment model parameters: Implications for climate impact analyses, Water Resources Research, 47, n/a-n/a, 10.1029/2010wr009505, 2011.

Mirza, M. M. Q., Warrick, R. A., Ericksen, N. J., and Kenny, G. J.: Trends and persistence in precipitation in the Ganges, Brahmaputra and Meghna river basins, Hydrological Sciences-Journal, 43, 345-858, 1998.

Mirza, M. M. Q.: Global warming and changes in the probability ofoccurrence of floods in Bangladesh and implications, Global Environmental Change, 127–138, 2002.

Mirza, M. M. Q.: Three Recent Extreme Floods in Bangladesh: A Hydro-Meteorological Analysis, Natural Hazards, 28, 35-64, 10.1023/A:1021169731325, 2003.

Mirza, M. M. Q., Warrick, R. A., and Ericksen, N. J.: The implications of climate change on floods of the Ganges, Brahmaputra and Meghna rivers in Bangladesh, Climate Change, 287-318, 2003.

Mirza, M. M. Q., and Ahmad, Q. K.: Climate Change And Water Resources In South Asia, edited by: edited by M. Monirul Qader Mirza, Q. K. A., A. A. Balkema Publishers, Leiden, Netherlands, 2005b.

Mizuta, R., Yoshimura, H., Murakami, H., Matsueda, M., Endo, H., Ose, T., Kamiguchi, K., Hosaka, M., Sugi, M., Yukimoto, S., Kusunoki, S., and Kitoh, A.: Climate Simulations Using MRI-AGCM3.2 with 20-km Grid, Journal of the Meteorological Society of Japan, 90A, 233-258, 10.2151/jmsj.2012-A12, 2012.

Nash, J. E., and Sutcliffe, J. V.: River flow forecasting through conceptual models part I – a discussion of principles, J. Hydrol., 10, 282–290, 1970.

NEO: Vegetation Index [NDVI] (1 Month - Terra/Modis), available at: http://neo.sci.gsfc.nasa.gov/view.php?datasetId=MOD13A2_M_NDVI&year=2000 (last access date: 19 April 2014), 2014.

Nishat, A., and Faisal, I. M.: An assessment of the Institutional Mechanism for Water Negotiations in the Ganges–Brahmaputra–Meghna system, International Negotiations, 289–310, 2000.

Nishat, B., and Rahman, S. M. M.: Water Resources Modeling of the Ganges-Brahmaputra-Meghna River Basins Using Satellite Remote Sensing Data, JAWRA Journal of the American Water Resources Association, 45, 1313-1327, 10.1111/j.1752-1688.2009.00374.x, 2009.

Oki, T., and Sud, Y. C.: Design of Total Runoff Integrating Pathways (TRIP)-A Global River Channel Network, Earth Interactions, 2, 1998.

Pfly: Ganges-Brahmaputra-Meghna basins.jpg: http://en.wikipedia.org/wiki/File:Ganges-Brahmaputra-Meghna_basins.jpg#, last access: April-2014, 2011.

Pokhrel, Y., Hanasaki, N., Koirala, S., Cho, J., Yeh, P. J. F., Kim, H., Kanae, S., and Oki, T.: Incorporating Anthropogenic Water Regulation Modules into a Land Surface Model, Journal of Hydrometeorology, 13, 255-269, 10.1175/jhm-d-11-013.1, 2012.

Rahman, M. M., Ferdousi, N., Sato, Y., Kusunoki, S., and Kitoh, A.: Rainfall and temperature scenario for Bangladesh using 20 km mesh AGCM, International Journal of Climate Change Strategies and Management, 4, 66-80, 10.1108/17568691211200227, 2012.

Sevat, E., and Dezetter, A.: Selection of calibration objective functions in the context of rainfall-runoff modeling in a Sudanese savannah area, Hydrological Sci. J., 36, 307-330, 1991.

Shaaban, A. J., Amin, M. Z. M., Chen, Z. Q., and Ohara, N.: Regional Modeling of Climate Change Impact on Peninsular Malaysia Water Resources, Journal of Hydrologic Engineering, 16, 1040-1049, 10.1061/(asce)he.1943-5584, 2011.

Siderius, C., Biemans, H., Wiltshire, A., Rao, S., Franssen, W. H., Kumar, P., Gosain, A. K., van Vliet, M. T., and Collins, D. N.: Snowmelt contributions to discharge of the Ganges, The Science of the total environment, 468-469 Suppl, S93-S101, 10.1016/j.scitotenv.2013.05.084, 2013.

Taylor, K. E., Stouffer, R. J., and Meehl, G. A.: An overview of CMIP5 and the experimental design, Bull Am Meteorol Soc, 93, 485–498, 10.1175/BAMS-D-11-00094.1, 2012.

Tateishi, R., Hoan, N. T., Kobayashi, T., Alsaaideh, B., Tana, G., and Phong, D. X.: Production of Global Land Cover Data – GLCNMO2008, Journal of Geography and Geology, 6, 10.5539/jgg.v6n3p99, 2014.

Thompson, J. R., Green, A. J., and Kingston, D. G.: Potential evapotranspiration-related uncertainty in climate change impacts on river flow: An assessment for the Mekong River basin, Journal of Hydrology, 510, 259-279, 10.1016/j.jhydrol.2013.12.010, 2014.

Tripp, D. R., and Niemann, J. D.: Evaluating the parameter identifiability and structural validity of a probability-distributed model for soil moisture, Journal of Hydrology, 93-108, 10.1016/j.jhydrol.2008.01.028, 2008.

Vaze, J., Post, D. A., Chiew, F. H. S., Perraud, J. M., Viney, N. R., and Teng, J.: Climate non-stationarity – Validity of calibrated rainfall–runoff models for use in climate change studies, Journal of Hydrology, 394, 447-457, 10.1016/j.jhydrol.2010.09.018, 2010

Wagener, T., McIntyre, N., Lees, M. J., Wheater, H. S., and Gupta, H. V.: Towards reduced uncertainty in conceptual rainfall-runoff modelling: dynamic identifiability analysis, Hydrological Processes, 17, 455-476, 10.1002/hyp.1135, 2003.

Weedon, G. P., Gomes, S., Viterbo, P., Österle, H., Adam, J. C., Bellouin, N., Boucher, O., and Best, M.: The watch forcing data 1958-2001: A meteorological forcing dataset for land surface- and hydrological-models.22, 1-41, 2010.

Weedon, G. P., Gomes, S., Viterbo, P., Shuttleworth, J., Blyth, E., Osterle, H., Adam, J. C., Bellouin, N., Boucher, O., and Best, M.: Creation of the WATCH Forcing Data and its use to assess global and regional reference crop evaporation over land during the twentieth century, J. Hydrometeorol, 12, 823–848, 10.1175/2011JHM1369.1, 2011.

Yatagai, A., Kamiguchi, K., Arakawa, O., Hamada, A., Yasutomi, N., and Kitoh, A.: APHRODITE: Constructing a Long-Term Daily Gridded Precipitation Dataset for Asia Based on a Dense Network of Rain Gauges, Bulletin of the American Meteorological Society, 93, 1401-1415, 10.1175/BAMS-D-11-00122.1, 2012.

Table 1: Major characteristics of the Ganges, Brahmaputra and Meghna River basin

Item		Brahmaputra	Ganges	Meghna
Origin and major properties [a]		The Brahmaputra River begins in the glaciers of the Himalayas and travels through China, Bhutan, and India before emptying into the Bay of Bengal in Bangladesh. It is snow-fed braided river and it remains a natural stream with no major hydraulic structures built along its reach.	The Ganges River originates at the Gangotri glaciers in the Himalayas and it passes through Nepal, China, and India and empties into the Bay of Bengal at Bangladesh. It is snowmelt-fed river regulated by upstream India.	The Meghna River is a comparatively smaller, rain-fed, and relatively flashier river that runs through a mountainous region in India before entering Bangladesh.
Basin area (km^2)		583 000[b] 530 000[f,g] 543 400[h]	907 000[b] 1 087 300[h] 1 000 000[c]	65 000[b] 82 000[h]
River length (km)		1 800[b] 2 900[f] 2 896[a]	2 000[b] 2 510[c] 2 500[a]	946[b]
Elevation (m a.s.l.) [e]	Range	8 ~ 7057	3 ~ 8454	-1 ~ 2579
	Average	3141	864	307
	Area below 500 m:	20%	72%	75%
	Area above 3000 m:	60%	11%	0%
Discharge ($m^3 s^{-1}$)	Station	Bahadurabad	Hardinge bridge	Bhairab bazar
	Lowest	3 430[d]	530[d]	2[d]
	Highest	102 535[d]	70 868[d]	19 900[d]
	Average	20 000[g]	11 300[d]	4 600[d]
Land use (% area)[i]	Agriculture	19%	68%	27%
	Forest	31%	11%	54%
Basin-averaged Normalized Difference Vegetation Index (NDVI)[j]		0.38	0.41	0.65
Total number of dams (both for hydropower and irrigation purpose)[k]		6	75	-

[a] Moffitt et al. (2011)
[b] Nishat and Faisal (2000)
[c] Abrams (2003)
[d] BWDB (2012)
[e] Estimated from SRTM DEM data by Lehner et al. (2006)
[f] Gain et al. (2011)
[g] Immerzeel (2008)
[h] FAO-AQUASTAT (2014)
[i] Estimated from Tateishi et al. (2014)
[j] Estimated from NEO (2014)
[k] Lehner et al. (2008)

1 Table 2. Basic input data used in this study

2

Type	Description	Source/Reference(s)	Original spatial resolution	Period	Remarks
Physical Data	Digital Elevation Map (DEM)	HydroSHEDS[a] (HydroSHEDS, 2014)	15″ (~0.5 km)	-	Global data
	Basin mask	HydroSHEDS[a] (HydroSHEDS, 2014)	30″ (~1 km)	-	
Meteorological data	rainfall, snowfall, surface pressure, air temperature, specific humidity, wind speed, long-wave downward radiation, shortwave downward radiation	WFD[b] (Weedon et al., 2010;Weedon et al., 2011)	0.5°	1980-2001	5′ (~10 km-mesh) data has been prepared by linear interpolating for this study
	albedo	GSWP2[c]	1°	1980-1990	Mean monthly 5′ (~10 km-mesh) data has been prepared for this study
Hydrologic data	water level discharge	Bangladesh Water Development Board (BWDB)	Gauged	1980-2012	water level (daily), discharge (weekly) data at outlets of three basins, i.e. the Ganges basin at Hardinge Bridge, the Brahmaputra basin at Bahadurabad, and the Meghna basin at Bhairab Bazar obtained from BWDB.
	discharge	Global Runoff Data Centre (GRDC)	Gauged	1949-1973 (Farakka), 1975-1979 (Pandu), 1969-1992 (Teesta) with missing data	discharge (monthly) data at three upstream stations, i.e. at Farakka (Ganges), Pandu (Brahmaputra) and Teesta (Brahmaputra).
GCM data	rainfall, snowfall, surface pressure,	MRI-AGCM3.2S[d]	0.25° (~20 km-	1979-2003,	bias of precipitation dataset has been corrected by

air temperature, specific humidity, wind speed, long-wave downward radiation, shortwave downward radiation		mesh)	2015-2039,2075-2099	multiplying using monthly correction coefficient (ratio between basin averaged long term monthly mean precipitation from WFD and that from each GCM) for each GBM basins
	MIROC5	1.41×1.39°		
	MIROC-ESM	2.81×2.77°		
	MRI-CGCM3	1.125×1.11°		
	HadGEM2-ES	1.875×1.25°		

[a]HydroSHEDS is Hydrological data and maps based on SHuttle Elevation Derivatives at multiple Scales,

[b]WFD is WATCH forcing data,

[c]GSWP2 is Second Global Soil Wetness Project,

[d]MRI-AGCM is Meteorological Research Institute-Atmospheric General Circulation Model

Table 3. Basic information of the streamflow validation stations in the GBM basins

Basin name	Brahmaputra			Ganges		Meghna
Station name	Bahadurabad	Pandu	Teesta	Hardinge bridge	Farakka	Bhairab bazar
Latitude	25.18° N	26.13° N	25.75° N	24.08° N	25° N	25.75° N
Longitude	89.67° E	91.7° E	89.5° E	89.03° E	87.92° E	89.5° E
Drainage area (km^2)	583 000	405 000	12 358	907 000	835 000	65 000
Available observed data period (with missing)	1980-2001	1975-1979	1969-1992	1980-2001	1949-1973	1980-2001

Table 4. The 22-year (1980-2001) averages of the meteorological (from the WFD forcing data) and hydrologic variables in the GBM river basins.

	Unit	Brahmaputra	Ganges	Meghna
(a) Meteorological variables				
Precipitation (Prcp)	mm $year^{-1}$	1609	1157	3212
Temperature (Tair)	°C	9.1	21.7	23.0
Net radiation (Net rad)	W m^{-2}	31	74	84
Specific humidity	g/kg	9.3	11.8	14.4
(b) Hydrological variables				
Runoff	mm $year^{-1}$	1360	406	2193
Evapotranspiration (ET)	mm $year^{-1}$	251	748	1000
Potential Evapotranspiration (PET)	mm $year^{-1}$	415	2359	1689

Table 5. The 10-simulation average of annual mean and percentage changes of hydrological and meteorological variables.

Variable	Period	Brahmaputra				Ganges				Meghna			
		annual mean	% change (Tair: °C)			annual mean	% change (Tair: °C)			annual mean	% change (Tair: °C)		
			dry season (November-April)	wet season (May-October)	annual		dry season (November-April)	wet season (May-October)	annual		dry season (November-April)	wet season (May-October)	annual
(a) Meteorological variables													
Pricipitation (mm year^{-1})	present-day (1979-2003)	1632	-	-	-	1154	-	-	-	3192	-	-	-
	near-future (2015-2039)	1720	4.2	5.6	5.4	1218	-0.1	6.2	5.6	3598	11.4	12.9	12.7
	far-future (2075-2099)	1897	23.0	15.1	16.3	1383	3.6	21.5	19.8	4139	33.6	29.0	29.6
Tair (°C)	present-day (1979-2003)	5.5	-	-	-	21.7	-	-	-	23.0	-	-	-
	near-future (2015-2039)	6.7	1.4	1.0	1.2	22.8	1.1	0.9	1.0	23.7	0.8	0.6	0.7
	far-future (2075-2099)	10.3	5.5	4.1	4.8	25.9	4.6	3.7	4.1	26.8	4.3	3.4	3.8
Net radiation (W m^{-2})	present-day (1979-2003)	63	-	-	-	97	-	-	-	114	-	-	-
	near-future (2015-2039)	62	2.0	-1.6	-0.4	97	-0.2	-0.9	-0.7	112	-0.4	-2.2	-1.5
	far-future (2075-2099)	66	10.3	3.1	5.6	101	5.3	3.4	4.1	119	6.5	3.0	4.4
(b) Hydrological variables													
Total runoff (mm year^{-1})	present-day (1979-2003)	1166	-	-	-	372	-	-	-	1999	-	-	-
	near-future (2015-2039)	1244	0.5	8.6	6.7	414	2.5	12.1	11.3	2380	10.5	20.2	19.1
	far-future (2075-2099)	1355	2.9	20.3	16.2	495	-2.3	36.3	33.1	2793	24.2	41.8	39.7
ET (mm year^{-1})	present-day (1979-2003)	467	-	-	-	785	-	-	-	1193	-	-	-
	near-future (2015-2039)	477	5.5	0.9	2.1	808	4.9	2.1	3.0	1216	5.2	0.4	1.9
	far-future (2075-2099)	543	25.6	12.9	16.4	892	19.3	10.9	13.6	1347	18.2	10.5	12.9
Soil moisture (mm)	present-day (1979-2003)	335	-	-	-	186	-	-	-	336	-	-	-
	near-future (2015-2039)	338	0.4	1.2	0.9	192	2.7	3.4	3.1	354	6.6	5.1	5.5
	far-future (2075-2099)	340	0.2	2.3	1.5	197	0.4	8.3	5.8	359	6.7	6.9	6.9

Table 6. Statistical indices (the coefficient of variation (CV) and standard deviation (SD)) of the uncertainty in model simulations due to the uncertainty in model parameters

Variable	Period	Brahmaputra		Ganges		Meghna	
		Coefficient of variation (CV) of mean (Fig.8) (%)	Standard deviation (SD) of mean (Fig.8)	Coefficient of variation (CV) of mean (Fig.8) (%)	Standard deviation (SD) of mean (Fig.8)	Coefficient of variation (CV) of mean (Fig.8) (%)	Standard deviation (SD) of mean (Fig.8)
Net radiation	present-day	8.6	5.4	2.0	2.0	2.1	2.4
	near-future	8.6	5.4	1.9	1.9	2.1	2.3
	far-future	8.4	5.6	1.8	1.8	2.0	2.4
Total runoff	present-day	3.2	0.1	7.6	0.1	6.7	0.4
	near-future	3.0	0.1	7.2	0.1	5.4	0.4
	far-future	3.1	0.1	6.6	0.1	4.6	0.4
ET	present-day	7.9	0.1	3.6	0.1	11.3	0.4
	near-future	7.9	0.1	3.7	0.1	10.6	0.4
	far-future	7.8	0.1	3.7	0.1	9.7	0.4
Soil moisture	present-day	31.0	103.7	18.5	34.5	15.9	53.5
	near-future	30.8	104.1	18.5	35.5	15.4	54.5
	far-future	30.5	103.7	18.3	36.1	14.4	51.6

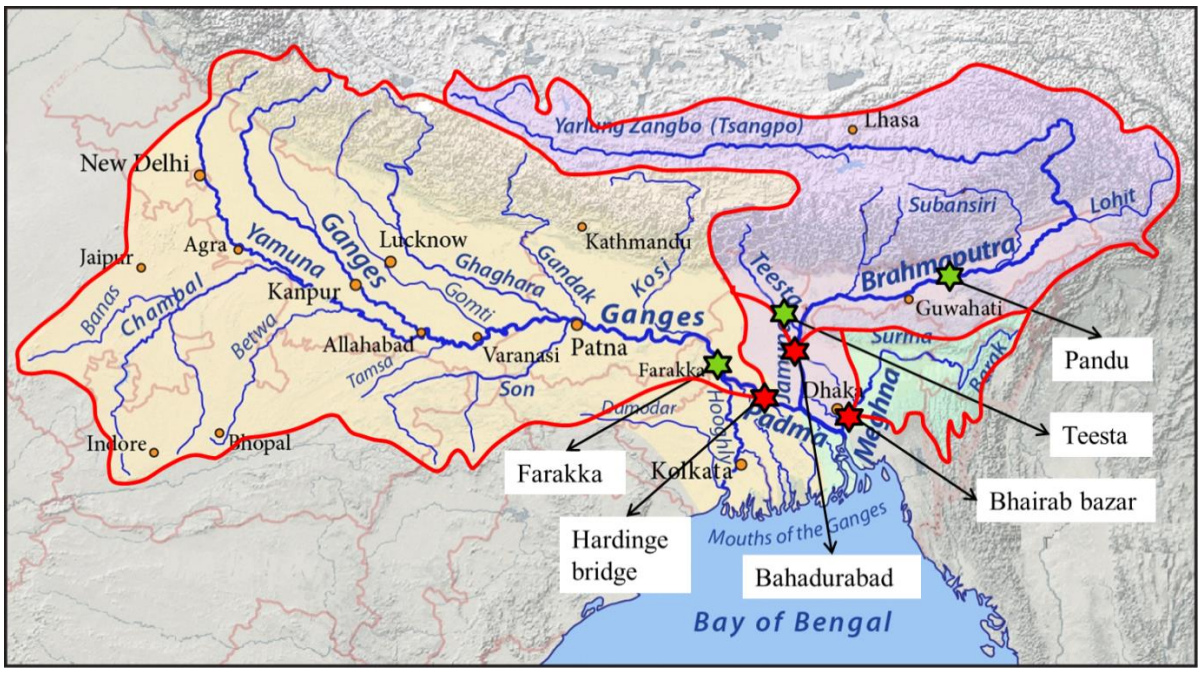

Figure 1. The boundary of the Ganges-Brahmaputra-Meghna (GBM) River basin (thick red line), the three outlets (red star): Hardinge bridge, Bahadurabad and Bhairab bazar for the Ganges, Brahmaputra and Meghna River basin, respectively. Green stars indicate the locations of three additional upstream stations; Farakka, Pandu and Teesta. (modified from Pfly, 2011).

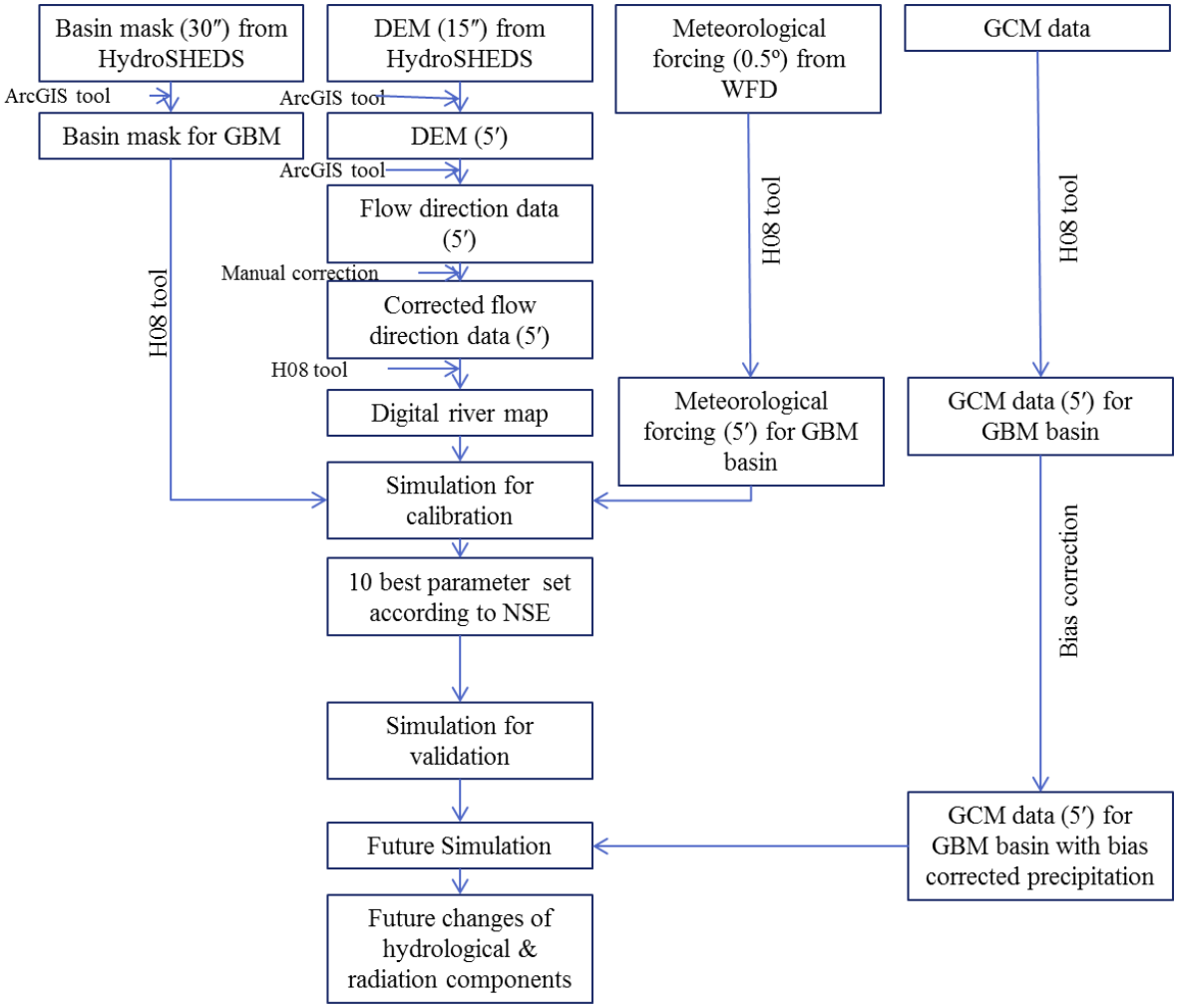

Figure 2. Flow chart of the methodology used in this study.

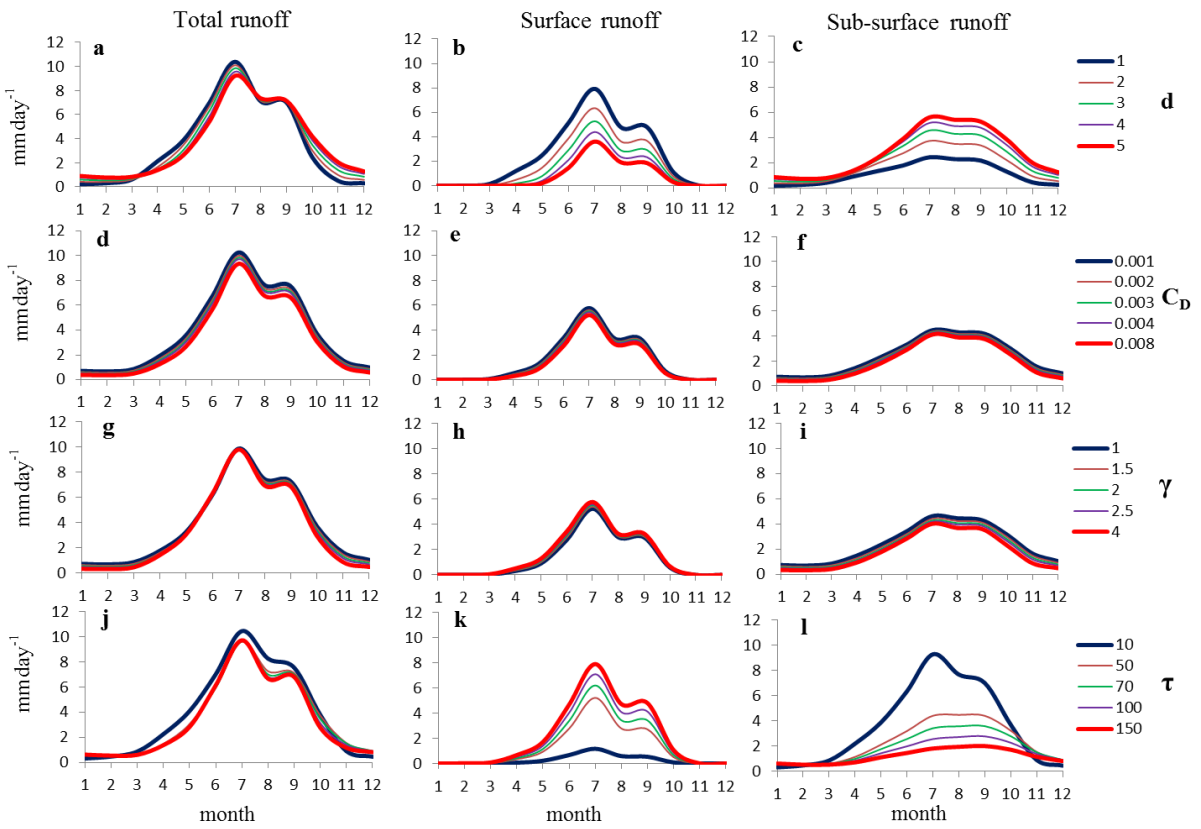

Figure 3. The 11-year (1980–1990) mean seasonal cycles of the simulated total runoff, surface runoff and sub-surface runoff (unit: mm day^{-1}) in the Brahmaputra basin. Each of the five lines in each panel represents the average of 5^3 (=125) runs with one of the four calibration parameters fixed at a given reasonable value.

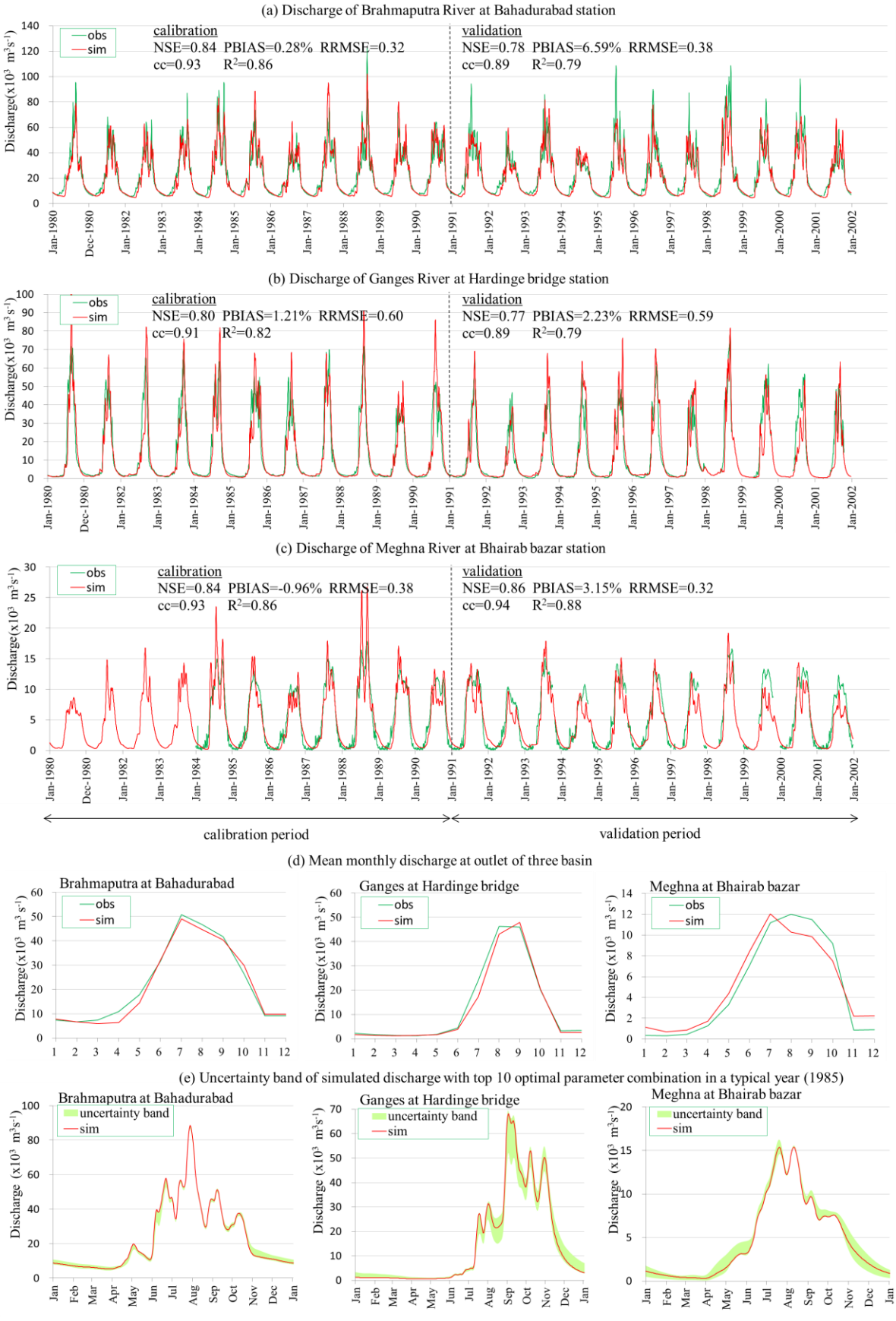
(a) Discharge of Brahmaputra River at Bahadurabad station
obs
sim
calibration
NSE=0.84 PBIAS=0.28% RRMSE=0.32
cc=0.93 R²=0.86
validation
NSE=0.78 PBIAS=6.59% RRMSE=0.38
cc=0.89 R²=0.79
Discharge(x10³ m³s⁻¹)
(b) Discharge of Ganges River at Hardinge bridge station
calibration
NSE=0.80 PBIAS=1.21% RRMSE=0.60
cc=0.91 R²=0.82
validation
NSE=0.77 PBIAS=2.23% RRMSE=0.59
cc=0.89 R²=0.79
(c) Discharge of Meghna River at Bhairab bazar station
calibration
NSE=0.84 PBIAS=-0.96% RRMSE=0.38
cc=0.93 R²=0.86
validation
NSE=0.86 PBIAS=3.15% RRMSE=0.32
cc=0.94 R²=0.88
calibration period
validation period
(d) Mean monthly discharge at outlet of three basin
Brahmaputra at Bahadurabad
Ganges at Hardinge bridge
Meghna at Bhairab bazar
(e) Uncertainty band of simulated discharge with top 10 optimal parameter combination in a typical year (1985)
uncertainty band
sim

Figure 4. The simulated discharges (red line) using the WFD forcing data (both calibration and validation period) compared with observations (green line) at outlets of the (a) Brahmaputra, (b) Ganges, (c) Meghna River, (d) mean monthly (1980-2001) simulated discharges compared with that of observations at outlets, (e) simulated discharges by using the 10 optimal parameter sets (red line) and the associated uncertainty bands (green shading) in a typical year (1985). Nash–Sutcliffe efficiency (NSE), percent bias (PBIAS), relative Root-Mean Square Error (RRMSE), correlation coefficient (cc) and coefficient of determination (R^2) for both calibration and validation period are noted at sub-plot (a), (b) and (c).

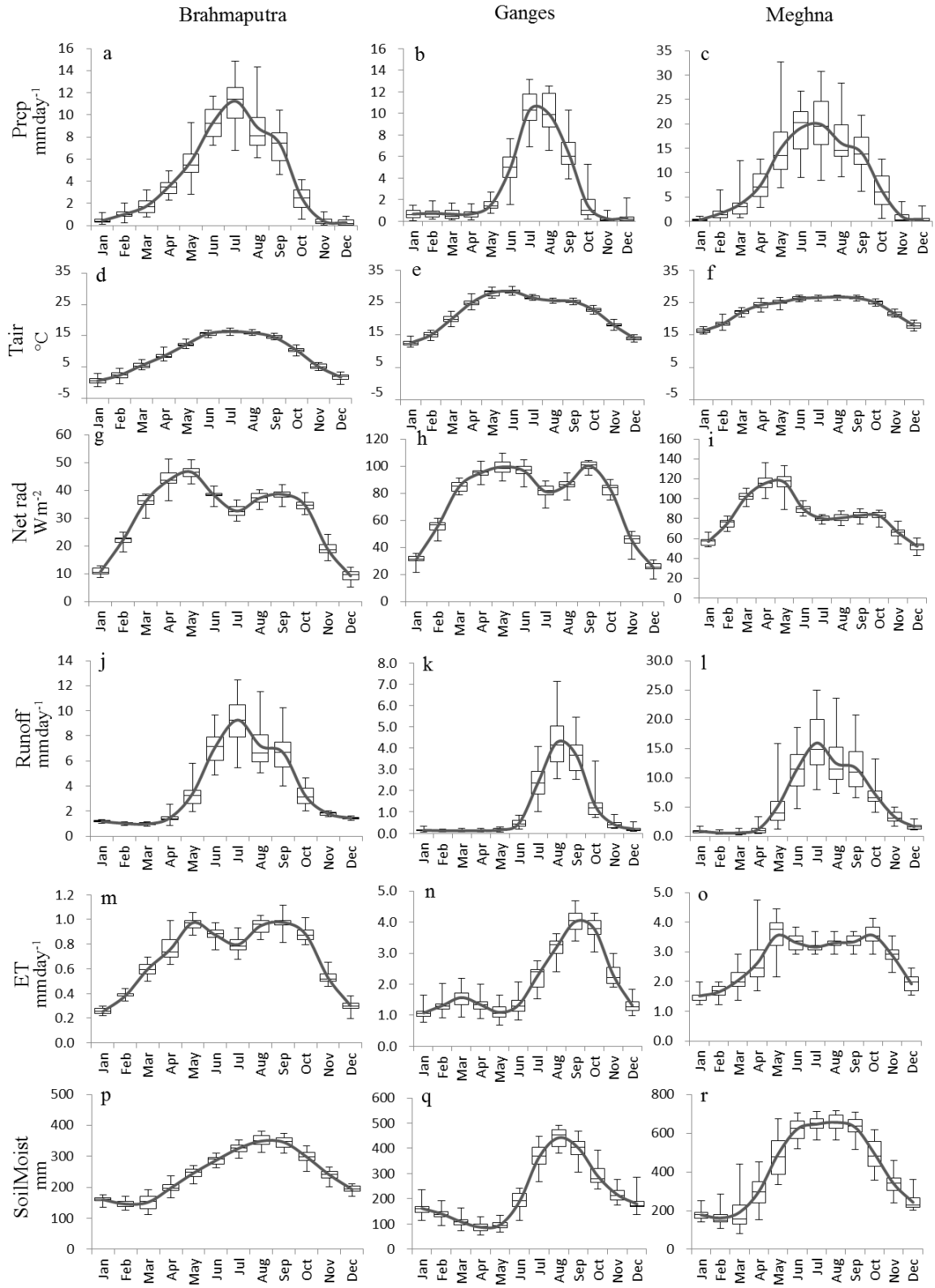

Figure 5 (a)-(r). Seasonal cycle of climatic and hydrologic quantities during 1980-2001. Box-and-whisker plots indicate minimum and maximum (whiskers), 25th and 75th percentiles (box ends), and median (black solid middle bar). Solid curve line represents interannual average value. All abbreviated terms here refer to Table 4.

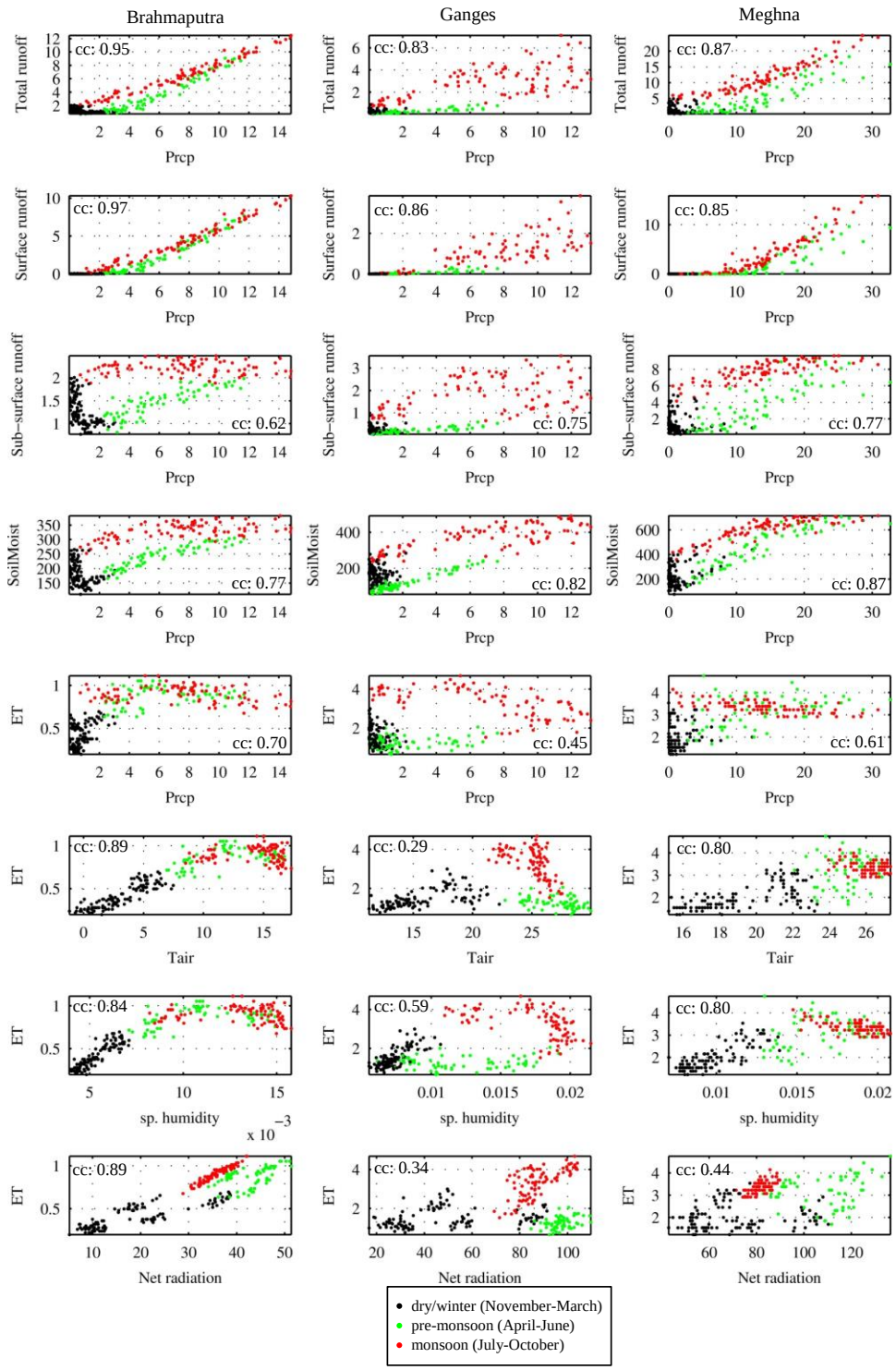

Figure 6. The correlation between the monthly means of meteorological variables (WFD) and that of hydrological variables for the Brahmaputra, Ganges and Meghna basins. Three different colors represent the data in three different seasons: Black: dry/winter (November-March); Green: pre-monsoon (April-Jun); Red: monsoon (July-October). The correlation coefficient (cc) for each pair (all 3 seasons together) is noted at each sub-plot. The units are mm day^{-1} for Prec, ET, runoff , mm for SoilMoist, °C for Tair, and W m^{-2} for net radiation. All abbreviated terms here are referred to Table 4.

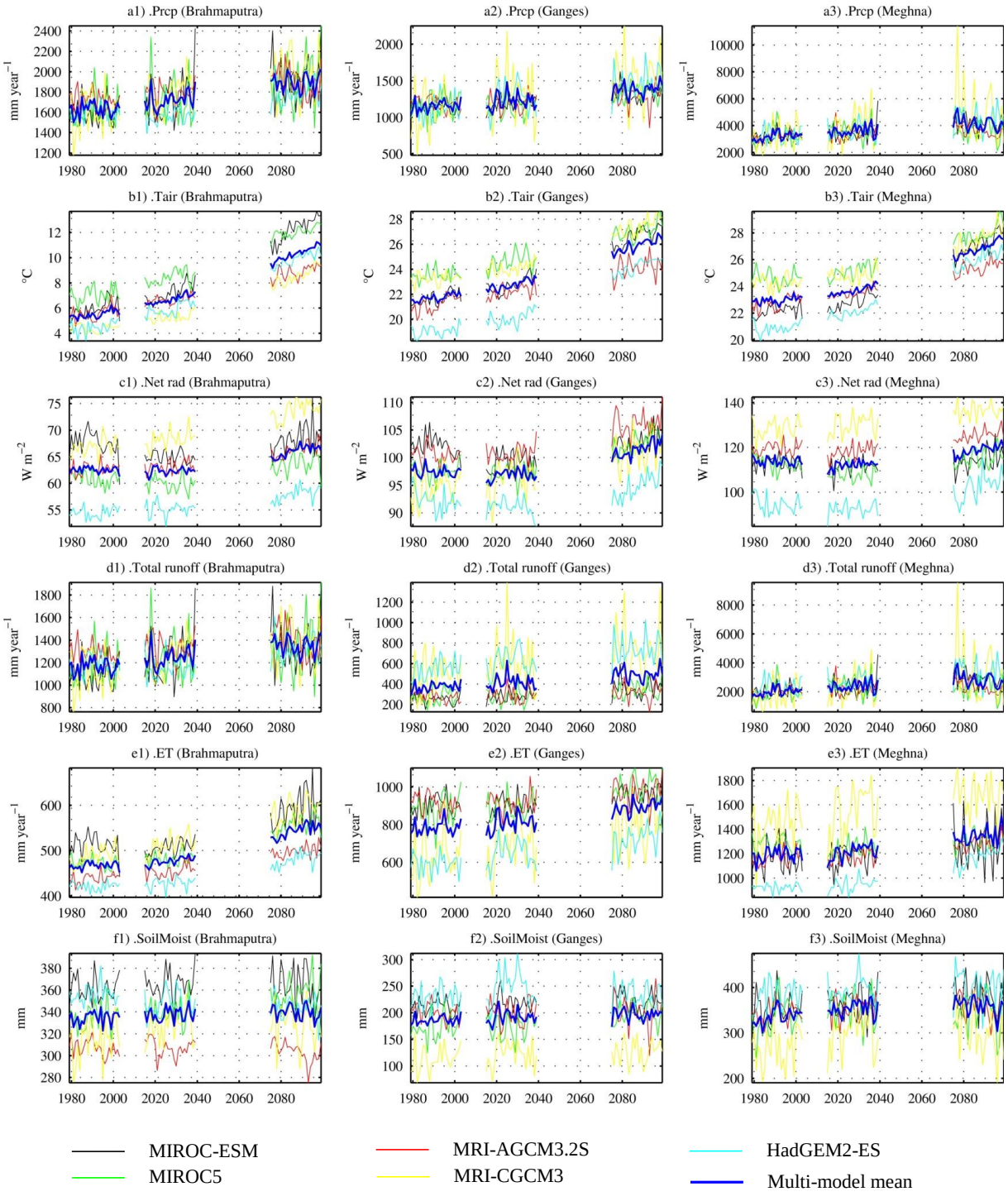

Figure 7 (a1-f3). Interannual variation of mean of meteorological and hydrological variables of 5 GCMs for present-day (1979-2003), near-future (2015-2039) and far-future (2075-2099). Thick blue lines represent the means of 5 GCMs.

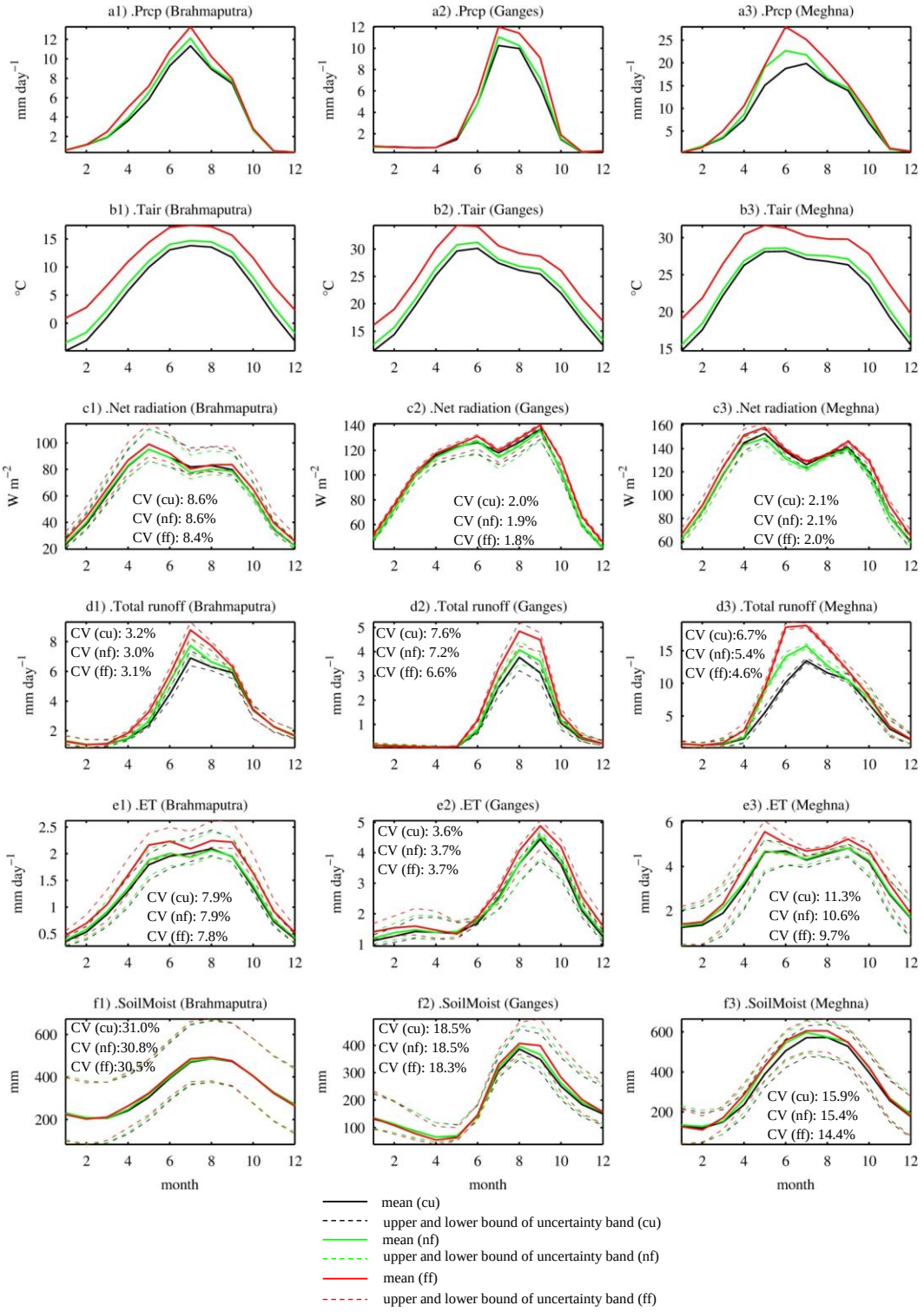

Figure 8 (a1)-(f3). The mean (solid line), upper and lower bounds (dashed line) of the uncertainty band of the hydrological quantities and net radiation components for the present-day (black), near-future (green) and far-future (red) simulations as determined found from 10 simulation result with considering 10 optimal parameter set according to Nash–Sutcliffe efficiency (NSE) (cu: present-day, nf: near-future, ff: far-future). Coefficient of variations (CV) for all periods (Table 6) are noted on each sub-plot.

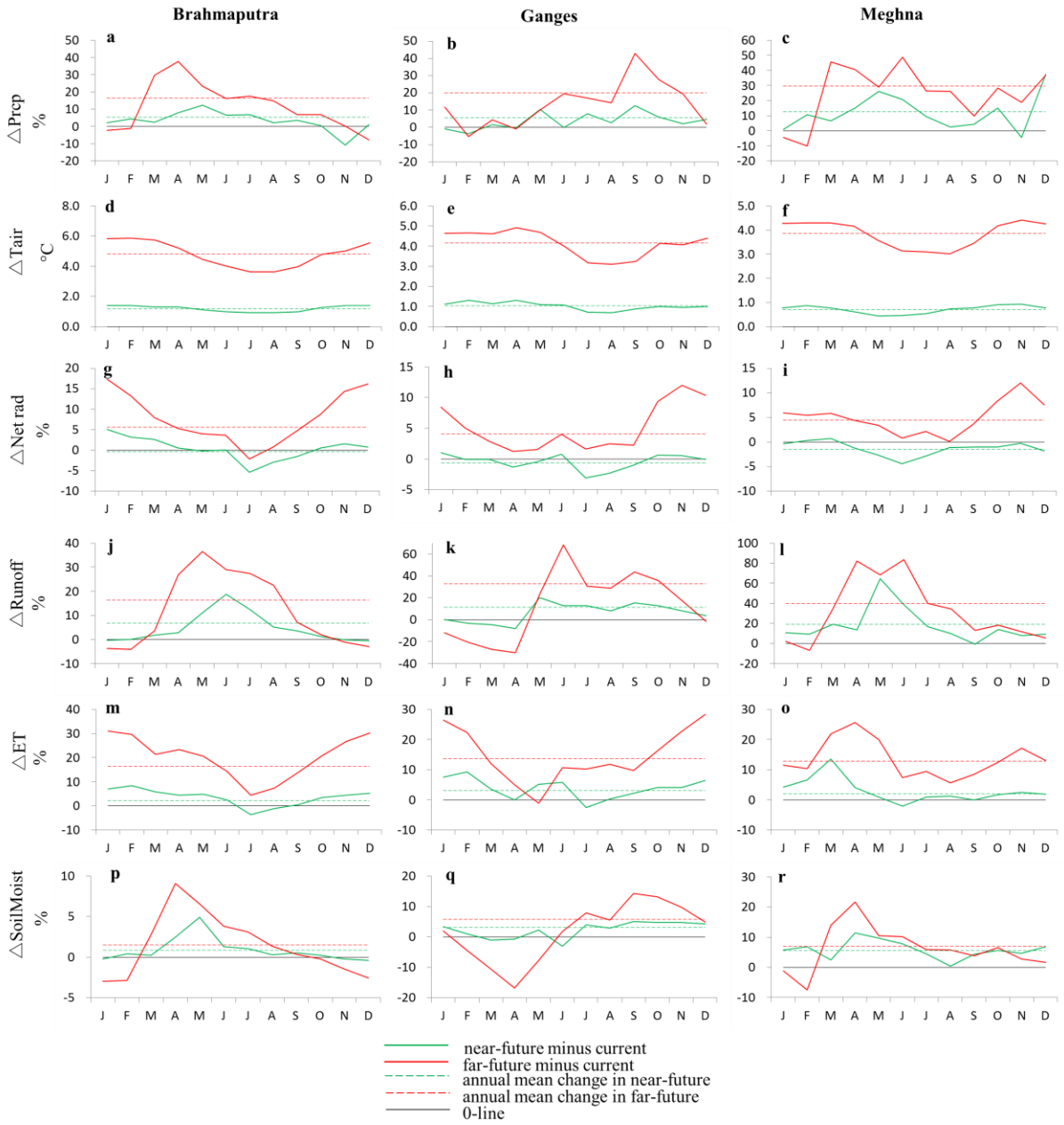

Figure 9 (a)-(r). Percentage changes in the monthly means of the climatic and hydrologic quantities from the present-day period to the near-future and far-future periods. The dashed lines represent the annual mean changes.

Appendix A: Model validation at three upstream station

The model performance was further evaluated by comparing the simulated monthly streamflow with the observed data from the Global Runoff Data Centre (GRDC) at three upstream gauging stations (Farakka, Pandu and Teesta) in the GBM basin. The locations and drainage areas of these three stations are summarized in Table 3. Although the available data period do not cover the study period 1980-2001 (except for the Teesta which has the data from 1985-1991), the mean seasonal cycle and the mean, maximum, minimum, and the standard deviation of the streamflow are compared in Figure A1 and Table A1. It can be seen that the mean seasonal cycle of simulated streamflow matches well with the corresponding GRDC data (Fig. A1d-f). Also the agreement of the simulated and observed 1985-1991 monthly streamflow at the Teesta station of the Brahmaputra basin is excellent (Fig. A1c).

Table A1. Comparison between observed (data source: GRDC) and simulated discharge ($m^3 s^{-1}$) at the Farakka gauging station in the Ganges basin, and Pandu and Teesta stations in the Brahmaputra basin.

Basin	Ganges		Brahmaputra		Brahmaputra	
Station	Farakka		Pandu		Teesta	
Data type	observed	simulated	observed	simulated	observed	simulated
Data period (with missing)	1949-1973	1980-2001	1975-1979	1980-2001	1969-1992	1980-2001
Mean	12 037	11 399	18 818	15 868	915	920
Maximum	65 072	69 715	49 210	46 381	3 622	4 219
Minimum	1 181	414	4 367	3 693	10	122
Standard deviation	14 762	15 518	12 073	11 709	902	948

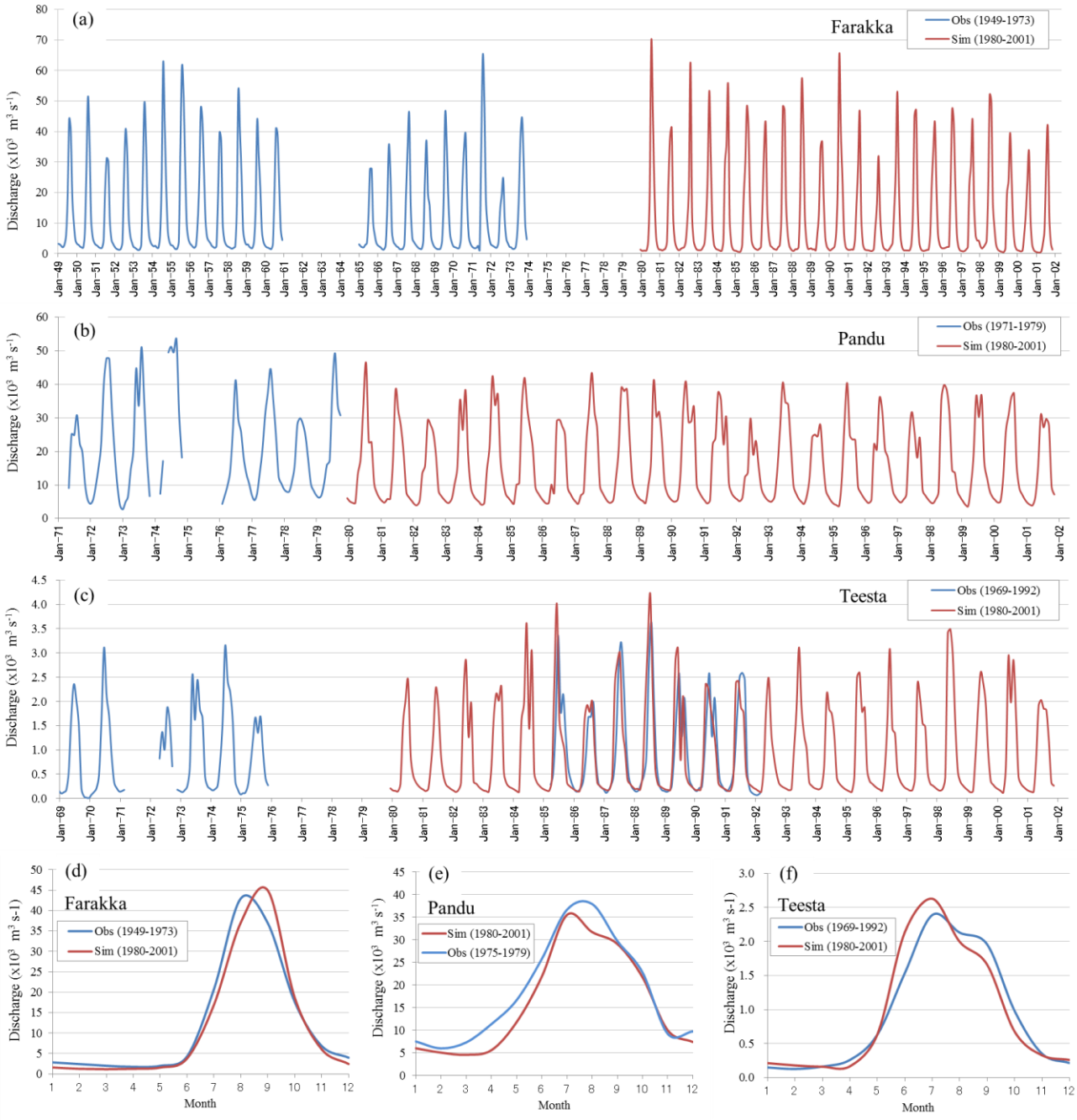

Figure A1. Comparisons between simulated (magenta line) and observed GRDC (blue line) data for (a-c) the monthly time series of discharges and (d-f) long-term mean seasonal cycles at the Farakka gauging station in the Ganges basin and the Pundu and Teesta stations in the Brahmaputra basin.

Appendix B:

Table B1: CMIP5 climate models used in the analysis

Model name	Modelling centre	Scenario	Nominal horizontal resolution
MIROC-ESM	Japan Agency for Marine-Earth Science and Technology, Atmosphere and Ocean Research Institute (The University of Tokyo), and National Institute for Environmental Studies	RCP 8.5	2.81 × 2.77°
MIROC5	Atmosphere and Ocean Research Institute (The University of Tokyo), National Institute for Environmental Studies, and Japan Agency for Marine-Earth Science and Technology	RCP 8.5	1.41×1.39°
MRI-AGCM3.2S	Meteorological Research Institute (MRI), Japan and Japan Meteorological Agency (JMA), Japan	SRES A1B	0.25×0.25°
MRI-CGCM3	Meteorological Research Institute (MRI), Japan	RCP 8.5	1.125× 1.11°
HadGEM2-ES	Met Office Hadley Centre, UK	RCP 8.5	1.875× 1.25°